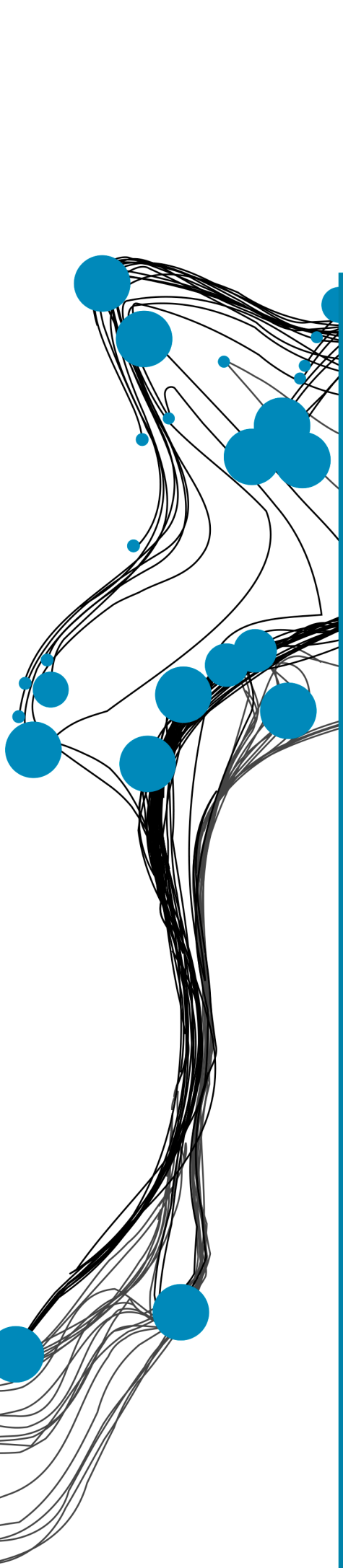

University of Twente

Department of Molecules and Materials

Bachelor Thesis

Biomedical Engineering

The influence of viscoelastic properties and surface roughnesses in an alginate-based hydrogel on the behaviour of hiPSC-CMs

Inge de Heer

November 20, 2023

The influence of viscoelastic properties and surface roughnesses in an alginate-based hydrogel on the behaviour of hiPSC-CMs

Inge de Heer

Molecular Nanofabrication
Prof. Dr. Ir. P. Jonkheijm

Examination committee

Overall supervisor:	Prof. Dr. Ir. P. Jonkheijm
Daily supervisor:	N. Debera
External member:	Prof. Dr. P.C.J.J. Passier

UNIVERSITY OF TWENTE. | MESA+ INSTITUTE | TECHMED CENTRE

Abstract

The extracellular matrix (ECM) significantly influences the behaviour of cells by mechanical and biochemical cues. An understanding of the role of these cues is necessary to create a suitable three-dimensional (3D) in vitro model that mimics the ECM of the native tissue, enabling cells to attach, spread and proliferate. Hydrogels are a class of biomaterials suitable for this application due to their high water content and biocompatibility. Here, a covalently crosslinked alginate-based hydrogel including RGD sequences was prepared and seeded with human-induced pluripotent stem cells derived from cardiomyocytes (hiPSC-CMs). Surface roughnesses were imparted by 3D printing a pattern onto the mould of the hydrogel. Since the covalently crosslinked hydrogel results in an elastic substrate and the embryonic cardiac tissue contains viscoelastic properties and exhibits stress relaxation, dynamic noncovalent bonds using cucurbit[8]uril and FGGC peptides were included. The storage modulus (G'), the loss modulus (G") and the stress relaxation were quantified and the influence of surface roughnesses was examined on the behaviour of the hiPSC-CMs. The results from this study demonstrate the role of the covalent crosslinking of the hydrogels and the presence of the dynamic bonds.

Nomenclature

Abbreviations

$2D$	Two-dimensional
$3D$	Three-dimensional
AB	Alamar Blue assay
$AEMA$	2-aminoethyl methacrylate
$ALGAEMA$	Alginate functionalised with 2-aminoethyl methacrylate
$C-RGD$	Cysteine-RGD
$CB[8]$	Cucurbit[8]uril
CM	Cardiomyocyte
ECM	Extracellular matrix
EDC	1-ethyl-3-(3-dimethylamino) propyl carbodiimide hydrochloride
FAC	Focal adhesion complex
$FGGC$	Phenylalanine-Glycine-Glycine-Cysteine
$hiPSC-CM$	Human induced Pluripotent Stem Cell Cardiomyocyte
PGs	Proteoglycans
RGD	Arginine-Glycine-Aspartic acid
$Sulfo-NHS$	sulfo-hydroxysuccinimide
UV	Ultraviolet

Symbols

ν	Poison's ratio
τ	Half relaxation time
E	Youngs modulus
G"	Loss modulus
G'	Storage modulus
G^*	Complex modulus

List of Figures

List of Tables

Contents

1 Introduction

In vitro, the development of functional cardiac tissue composed of human induced pluripotent stem cells derived from cardiomyocytes (hiPSC-CMs) and an extracellular matrix (ECM) holds significant promise as alternative substrates for cellular studies, such as toxicology and drug development. However, its potential applications remain constrained due to the highly organized nature of cardiac tissue, characterised by unique physiological, biomechanical, and electrical properties [1] and additionally, because current organ models are still mainly two-dimensional (2D). 2D models do not adequately represent human physiology and animal models pose issues of cost, time, ethics, and limited predictive capability. The emergence of three-dimensional (3D) models offers a promising alternative [2].

Morphology, cell adhesion and viability of the cells are influenced by the mechanical properties and physiological conditions of the ECM, which highlights the need to recapitulate these properties. For example, the incorrect rigidity of cell culture substrates frequently corresponds to various disease phenotypes, such as the transformation of fibroblasts into myofibroblasts in cardiac fibrosis [2]. In vivo, the dynamic mechanical microenvironment of the heart is viscoelastic and exhibits stress relaxation. This time-dependent response to deformation or mechanical load plays a crucial role in physological mechanisms [3][4].

Biomaterials to mimic the ECM, are natural substances that can engage with biological systems and maintain signalling. Using hydrogels is a suitable solution for this application. The 3D covalently crosslinked polymer network is highly hydrated and the mechanical properties of the hydrogels can be tuned across a broad spectrum. Since a covalently crosslinked hydrogel mainly results in elastic properties, the addition of dynamic bonds to the hydrogel can allow stress relaxation and promote more viscoelastic properties. Furthermore, proteins or peptide sequences of the ECM can be isolated and reconstructed to create hydrogels with a similar composition resembling that of various cellular microenvironments [2][5].

In this study, a functionalised hydrogel composed of alginate, AEMA, C-RGD and host-guest complexes of cucurbit[8]uril (CB[8]) and the peptides FGGC are used to recapitulate native cardiac ECM and promote hiPSC-CMs to attach and spread on top of the hydrogel. On the surface of the hydrogel, a pattern will be applied, which increases the perimeter of the surface and thus the space for the cells to spread and attach. The reason for this application is to study the behaviour of the cells and the response to these surface roughnesses. The morphology, viability and attachment of the cells in combination with the presence of different focal adhesion complexes and proteins, are executed using different measurements and imaging methods, such as the brightfield microscope, an Alamar Blue assay and immunostaining. The mechanical properties of the hydrogel, such as the elastic modulus (G'), the loss modulus (G") and the stress relaxation time are measured via rheology.

1.1 Aim of this research

This research aims to investigate the influence of viscoelastic properties and surface roughnesses in an alginate-based hydrogel on the behaviour of hiPSC-CMs to increase cell adhesion and survival. The aim is initially to determine how the dynamic bonds affect the elasticity and stress relaxation of the hydrogel, followed by an examination of cell behaviour on these hydrogels and hydrogels with applied surface roughnesses.

This research and experiments are part of a study aimed at establishing an in vitro model for investigating the (electrical) communication from pacemaker cells to CMs.

2 Theory

2.1 Cardiac tissue

The heart walls consist of three distinct layers; the endocardium, the myocardium and the epicardium. Each with its own properties and functions. The myocardium is the middle and thickest layer of the heart which functions as a cohesive unit and relies on electrochemical gradients to contract synchronized and generate the force required to provide blood throughout the entire body. The electrical impulses that set the rhythm and the rate of the heartbeat are generated by a cluster of myocytes with pacemaker activity, also known as the sinoatrial node (SAN) [2][6]. The remaining majority of the myocardium consists of myocardial contractile cells and the extracellular matrix (ECM). The myocardial contractile cells make up 99% of the cells in the ventricles and atria and are responsible for the pumping activity in the heart [6][7][8].

In this study, cardiomyocytes derived from human induced pluripotent stem cells (hiPSC-CMs) are used. Figure 1 illustrates how somatic cells are derived from healthy or diseased donors, reprogrammed into human induced pluripotent stem cells (hiPSCs) and differentiated into hiPSC-CMs. The immature hiPSC-CMs can mature into adult CMs, by controlling the cellular shape and the direct environment of the cells [9]. This potential of hiPSC-CM maturation is desired, since hiPSC-CMs can serve as a valuable new experimental model for investigating the physiology and diseases related to human cardiac muscle, but lack important machinery in terms of contractile function, mitochondria metabolism, organisation of sarcomeres and Ca^{2+} processing, compared to adult CMs [9][10].

Figure 1: Schematic overview of extracting somatic cells, such as skin fibroblasts or blood cells, reprogramming the somatic cells and differentiating into hiPSC-CMs. Created with BioRender.com

HiPSC-CMs exhibit thus an immature, fetal-like phenotype with a disorganized structure and contractile mechanics [11]. Figure 2 illustrates the misalignment of myofibrils in immature CMs compared to mature CMs, which influence the contractility activity. Furthermore, hiPSC-CMs typically exhibit a flat, circular morphology characterized by isotropic filament organization and a low expression of cytoskeletal proteins and ion channels [9][12].

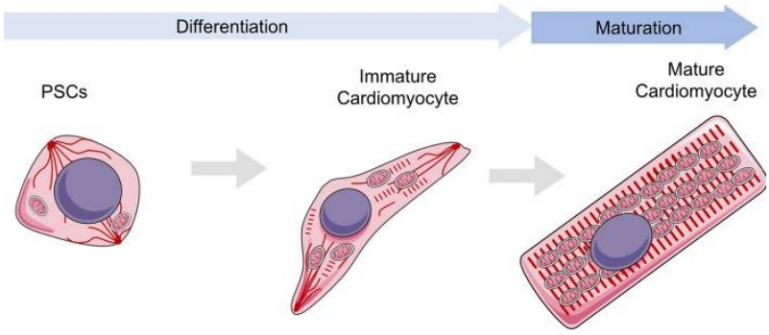

Figure 2: Schematic representation of the differentiation process of a pluripotent stem cell (PSC) to an immature cardiomyocyte and the maturation into a mature cardiomyocyte, highlighting the morphological and microstructure differences between immature and mature cardiomyocytes. The figure is adapted from Figure 1 in [13].

Adult ventricular cardiomyocytes are specialized, striated, single-nucleated muscle cells [14] and form a branching network connected by the membrane of the cells (sarcolemma) at intercalated discs (Figure 3a). The intercalated disc contains three junctional complexes; gap junctions, fascia adhera and desmosomes (Figure 3a). The gap junctions allow charged ions to pass between adjoining cells to enhance communication and maintain the electromechanical integrity of the heart and desmosomes and fascia adherens mechanically couple CMs prevent them from being pulled apart during contraction [6][8][15]. Cardiomyocytes possess large mitochondria, which provide energy for muscle contraction. The muscle contraction is created by the shortening and elongation of the myofibrils, consisting of the longitudinal repeating units, called sarcomeres [8].

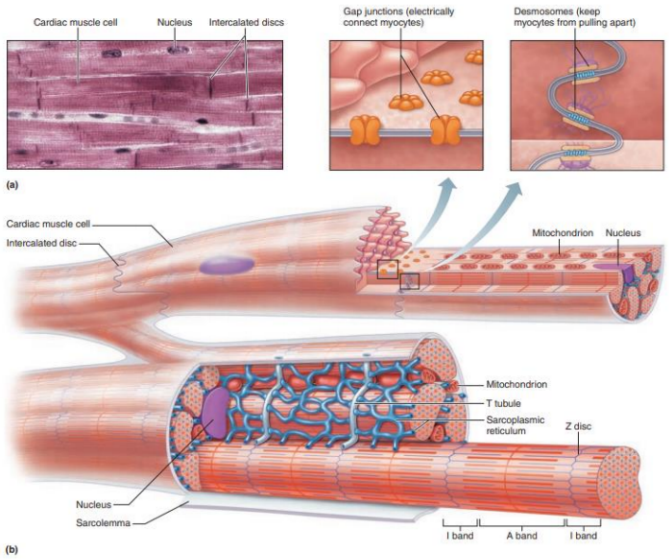

Figure 3: The cellular structure of the cardiac muscle at microscopic level. a) A Photomicrograph of cardiac muscle cells with dark-stained intercalated discs (290×). b) Anatomy of the cardiac muscle fibers and intercalated disc [8]

2.1.1 Cardiac ECM

The cardiac extracellular matrix (ECM) is the non-cellular component surrounding the cardiomyocytes and offers support and structural organization to maintain homeostasis in the heart. The ECM is secreted by the

surrounding cells and is formed by a complex mixture of fibrous proteins and proteoglycans (PGs). The composition of this mixture is critical for the behaviour of the cells in terms of adhesion, migration, proliferation and differentiation [16][17]. The fibrous proteins in the ECM are primarily collagens but also include fibronectins, laminins and elastins. Collagen is the most abundant protein in the ECM and imparts strength to the matrix. Fibronectin is secreted by various cell types such as cardiac fibroblasts and endothelial cells and serves as a cell adhesion protein. It mediates the cell-matrix interactions by binding to integrins and syndecans on the surface of the cell. Laminin forms a network and contains also an integrin-binding domain by which it can mediate cell adhesion. Elastin is known for its elasticity which imparts resilience to the matrix and allows it to return to its original shape after deformation [18]. Proteoglycans (PGs) are composed of glycosaminoglycan (GAG) chains, linked covalently to a specific protein core and adopt a hydrated gel-like form filling the majority of the extracellular interstitial space [19].

During embryonic development, the composition of the ECM undergoes constant dynamic changes. In the initial stage, the extracellular matrix of the myocardium primarily comprises an immature collagen III network, constituted by thin and loosely arranged fibers [11]. Collagen type III provides elasticity to the tissue [18]. The ECM develops gradually during the further embryonic phase with the distribution and expression of laminin and fibronectin and the increase of collagen fiber thickness. This process transforms the initial immature collagen network in the ECM, into a highly aligned, interconnected and interwoven network of collagen type I and III [11]. Collagen type I is a primary collagen that offers tensile strength and structural support [20].

The maturation and other cellular processes are largely dependent on the mechanical properties of the ECM since the cells interact with the ECM through dynamic processes, which are time-dependent and strain-dependent. The mechanical signals of the ECM will be transformed into biochemical signals and start mechanotransduction pathways in the cell, which inhibit or enhance genetic programs to control cell survival, fate and behaviour. Furthermore, the response of the ECM on the intrinsic forces produced by hiPSC-CM influences the behaviour of the cells as well. Cells detect substrate elasticity by measuring the resistance to the traction forces they apply on the substrate [21]. Figure 4 illustrates that intrinsic forces generated by cells induce deformation in substrates in a dynamic manner [22]. Optimal transmission of contraction, which promotes actomyosin striation and 1-Hz beating in immature hiPSCs, occurs when the substrate's elasticity matches that of the developing cardiac ECM [23]. Cardiac ECM exhibits viscoelastic properties, with an increasing elastic modulus with a higher state of maturity [24]. This is an important regulator of hiPSC-CM maturation since the force production of hiPSC-CMs relies on the resistance the cell encounters during contraction. Wheelwright et al. examined that the hiPSC-CMs produce significantly more force on a substrate with a modulus of 3.1 kPa than on a 9.8 or 13.5 kPa modulus substrate [25]. The elastic modulus of an adult and healthy heart ranges between 5 and 10 kPa [23].

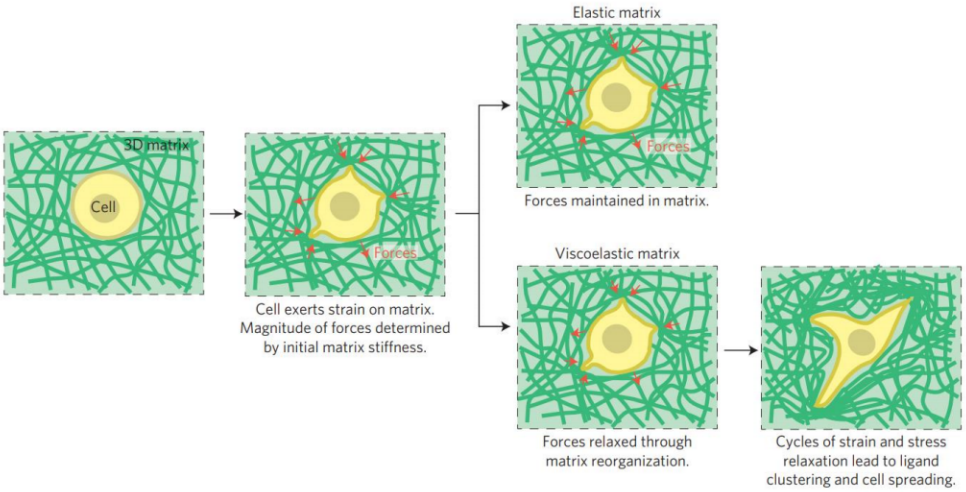

Figure 4: Possible cellular behaviour to initial elastic modulus and stress relaxation characteristics of the matrix [26].

2.1.2 Signalling pathways

The complex interplay between the ECM and cells is mainly enabled by the cell surface receptors, integrins and the proteins present in the ECM described in 2.1.1, called ligands. Integrins are transmembrane adhesion receptors that facilitate bi-directional communication through the membrane [11]. In cardiac tissue, the interaction between the ligands and the cytoskeleton through integrin receptors starts with integrin clustering and recruiting the proteins talin, α-actinin and vinculin. This complex of integrins, adapter proteins and the cytoskeleton is called the focal adhesion complex (FAC) and can transmit mechanical pressure and signals from CMs to the ECM and vice versa [27][28]. After FAC formation, actin polymerization occurs, by which individual actin monomers assemble into long chains or filaments and finally, the formation of actin-myosin stress fibers occurs, providing rigidity to the cell and establishing a mechanosensitive connection between the extracellular and intracellular environments. The mechanical force generated by the CMs through actomyosin-based contractility is translated to the ECM by coupling via integrin-based adhesions and the detection of substrate stiffness is mainly enabled through the magnitude and extent of FAC complexes [29].

2.2 Alginate based hydrogel

Alginate is primarily sourced from brown seaweeds and this naturally occurring polysaccharide stands out as a versatile and adaptable biomaterial, with biologically favourable properties, such as easy gelation and biocompatibility, which makes alginate-based hydrogel particularly appealing for cell encapsulation [30].

The structural integrity of the alginate-based hydrogel is highly tuneable and the mechanical properties can be adjusted by modifying various factors, such as the crosslinking density, network architecture and the addition of dynamic bonds. These are effective methods for controlling the viscoelastic properties of the hydrogel and allow mimicking the cardiac ECM. Furthermore, the high water content of the hydrogel creates a watery milieu and facilitates the effortless movement and diffusion of molecules secreted by the cells [5]. Alginate is an anionic polymer of monomers distributed as blocks of (1,4)-linked α-L-guluronate (G block) acid or βD-mannuronate (M block) acid as well as heteropolymeric mix sequences (G-M) [31][32][33].

Figure 5 shows the reaction, where sodium alginate is functionalized with a 2-aminoethyl methacrylate (AEMA) molecule. This methacrylate group enables UV-induced crosslinking with a photo-initiator and can react with

the cysteine side group of a peptide. 1-ethyl-3-(3-dimethylamino) propyl carbodiimide hydrochloride (EDC), which offers a better-leaving group to the reaction and sulfo-hydroxysuccinimide (sulfo-NHS), which improves the efficiency of the reaction, are the catalysts in this reaction and activate the carboxylic acid (-COOH) group of alginate. This enables the amino (NH2) of AEMA to carry out a nucleophilic attack on the ester, forming an amide bond and resulting in the molecule ALGAEMA [34].

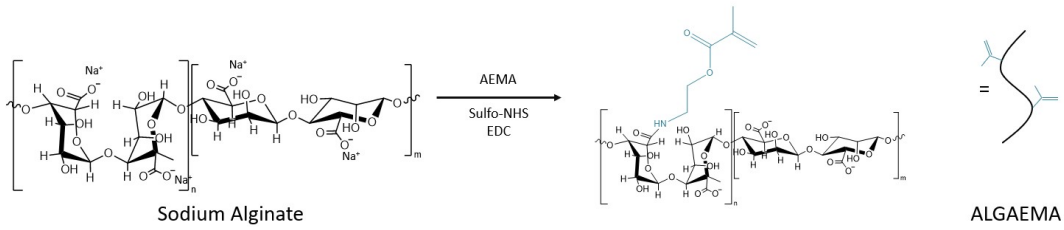

Figure 5: The chemical process of the activation of alginate with AEMA resulting in ALGAEMA including the schematic representation of ALGAEMA.

The crosslinking of the polymers is done using a photo-initiator and ultraviolet (UV) radiation. After exposure to UV, the photoinitiator compounds produce free radicals, which can initiate the polymerization process. The double bonds of the AEMA react, resulting in covalent crosslinked bonds between the polymers chains of the alginate[35].

2.2.1 Functionalization with the short C-RGD peptide

The polymers of the ALGAEMA hydrogel usually lack the inclusion of biological ligands necessary for direct interactions with cell surface receptors. As a strategy to create substrates that engage with cell surface receptors, the substrates need to be modified with functional fragments of ECM proteins, such as RGD-peptides [36]. The tripeptide Arg-Gly-Asp (RGD) is present in many adhesive proteins in the ECM, such as fibronectin, vitronectin and some laminins and is a cell recognition sequence for integrin receptors on the cell surface [32]. The specific amino acid sequence used in this research is CGGSGGSGGRGDSG and is derived from fibronectin. Figure 6 shows that the side group of the sequence is cysteine which includes a thiol (-SH) and can link through a Thiol Michael Addition reaction with the double bond of AEMA.

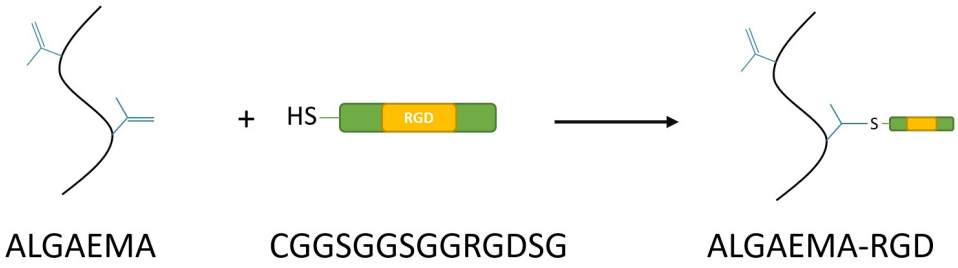

Figure 6: The Thiol Michael addition reaction of the double bond of AEMA and the thiol (-SH) side group of the RGD peptide sequence.

2.3 Mechanical properties

The conditions and degree of crosslinking and the selection and organisation of the polymers, such as the type and molecular weight of the constituents, are key factors in influencing the mechanical properties. The elasticity characterises the resistance of an object to undergo reversible deformation. A hydrogel with pure elastic properties is created through the establishment of a perfect covalent polymer and completely regains its initial shape after deformation induced by an external force, as it can store and recover all of the input deformation energy without any loss. Non-ideally crosslinked polymer networks, including unlinked polymers

and free ends, result in the dissipation of energy. The opposite characteristic of elasticity is viscous. Viscosity is a measure of a fluid's resistance to flow and deformation. Viscoelasticity thus means that the material undergoes some degree of viscous flow and/or permanent deformation, that leads to a time-dependent stress dissipation [22][35][37].

2.3.1 Rheology

Rheology is a suitable technique for dynamic and statical mechanical testing since it is sensitive and requires small sample sizes [38]. These methods characterize the macroscopic mechanical properties of materials such as the stiffness and viscosity of the materials. A time sweep is conducted, where the storage modulus (G') and the loss modulus (G") can be determined. Executing a stress relaxation test using rheology, the half relaxation time (τ = 1/2) of the hydrogel can be defined [37].

The storage modulus (G') in Pa describes the solid-state behaviour of the hydrogel and thus characterises the elastic portion of the viscoelastic behaviour by representing the stored deformation energy under cyclic loading. The loss modulus (G") represents the viscous portion of the viscoelastic behaviour by the material's ability to dissipate energy under cyclic loading [39]. The storage modulus and loss modulus are significant parameters utilized for characterizing the dynamic mechanical properties of materials. The Youngs modulus (E) is calculated following Formula 1 [40], with a Poisson's ratio (ν) of ν = 0.5 for alginate [31][39] and the complex modulus (G^*). G', G", G* and δ are related to each other using Formulas 2 and 3 [41], where the phase angle δ represents the time delay between the initial setup and the resulting sinusoidal oscillation and is determined for each measuring point [42]. The loss tangent ($\tan\delta$) is the ratio of G" to G' and indicates the degree of viscoelasticity. Soft tissues typically exhibit loss moduli ranging from 10% to 20% of their storage moduli at 1 Hz [22].

$$E = 2G^*(1+\nu) \tag{1}$$

$$G' = G^* Cos\delta \tag{2}$$

$$G" = G^* Sin\delta \tag{3}$$

Another parameter of the mechanical properties using rheology is stress relaxation. This time-dependent test illustrates how viscoelastic materials dissipate stress under a constant strain [43][44]. The time when the stress is half of its initial value is called the half relaxation time and provides insight into the capability of displacing water and rearranging the polymer network within the hydrogel. Hydrogels that exhibit stress relaxation, initially encounter a certain stiffness, followed by a decrease in resistance over time, when the cell applies a force or strain to the matrix. In hydrogels with weak crosslinks is relaxation partly a result of crosslink unbinding and hydrogel flow, allowing cellular forces to mechanically remodel the matrix [22]. Therefore, it is important to establish dynamic bonds in the covalently crosslinked ALGAEMA to allow cells to spread, proliferate and migrate within the hydrogel.

2.3.2 The presence of dynamic bonds

To mimic and improve the viscoelastic properties as well as structural stability, a host-guest system is added to the hydrogel, with a host named Cucurbit[8]uril (CB[8]), to include dynamic bonds besides the covalent and non-reversible bonds of the ALGAEMA crosslinked polymers (Figure 7). CB[8] is an effective and reversible crosslinker that can impart desirable dynamic properties. CB[8] is a family member of cucurbit[n] (where n represents the number of glycoluril units), it has a partly enclosed cavity which can simultaneously adopt two planar and hydrophobic guests. This capability enhances the hydrogel's responsiveness to cellular forces through disruption and re-establishment of crosslinking junctions [45]. The guest in the system is a side group of phenylalanine (F) of the peptide sequence FGGC (Phe-Gly-Gly-Cys). Through thiol-click chemistry, the end group of FGGC, cysteine reacts with the double bond of the methacrylate group. The inclusion of two

FGGC peptides in one CB[8] cavitand, improves the solubility of CB[8] in the physiological medium.

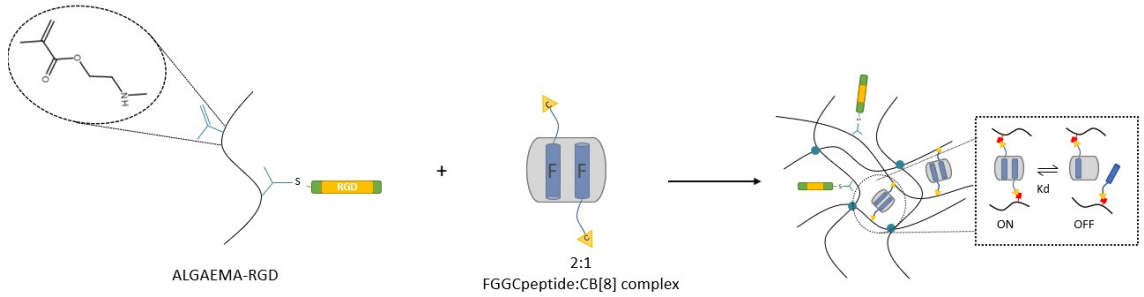

Figure 7: A schematic overview of the addition of the host-guest complex FGGC:CB[8] to the ALGAEMA-RGD polymers, resulting after crosslinking in a covalently crosslinked network of ALGEAMA-RGD and dynamic bonds of FGGC:CB[8] complexes.

3 Material and methods

3.1 ALGAEMA-RGD hydrogel preparation

Sodium alginate (FUJIFILM Wako Pure Chemical Corporation (Richmond, VA, U.S.A. Sodium Alginate 80-120)) was first functionalised with an aminoethyl methacrylate molecule (AEMA)(Sigma-Aldrich, St. Louis, MO, USA 516155) to obtain ALGAEMA [35]. The sodium alginate was activated with sulfo-NHS (Thermo Fisher Scientific, Waltham, MA, USA 24510)(sulfo-NHS : alginate = 0.7 : 1) and EDC (EDC : sulfo-NHS 2 : 1). The AEMA is added following the ratio (AEMA : alginate 0.3 : 1).

3.1.1 Addition of C-RGD

The RGD sequence CGGSGGSGGRGDSG (C-RGD), provided by the Molecular and Materials Chemistry group from CICA (Spain), was added to the ALGAEMA by a Thiol Michael Addition reaction. First, a solution of 1% w/v ALGAEMA in phosphate-buffered saline (PBS) was prepared in a glass beaker and left on a magnetic stirrer. 19 mg of C-RGD per 1 g of ALGAEMA was dissolved in PBS and slowly added drop-by-drop to the ALGAEMA solution while on the magnetic stirrer. Covered with aluminium foil, the solution was stirred for approximately 1h to a homogeneous solution. A dialysis membrane (MWCO of 3.5 kDa) was filled with the reacted ALGAEMA-C-RGD and dialysed against demi-water overnight to remove any unreacted C-RGD. The next day the product was frozen with liquid nitrogen and freeze-dried.

3.2 Hydrogel formation

To obtain 2% (w/v) ALGAEMA in the final hydrogels, initially 4% (w/v) ALGAEMA is dissolved in 0,1% (w/v) LAP (lithium phenyl-2,4,6-trimethylbenzoylphosphinate)(Sigma-Aldrich, St. Louis, MO, USA) and used to add different components to obtain variable conditions of the hydrogel. First, 4 mM of TCEP (tris-(2-carboxyethyl)fosfine)(Sigma-Aldrich, St. Louis, MO, USA) was dissolved in Milli-Q (2,29 mg TCEP per 1000 μL Milli-Q). The TCEP was added to break disulfide bonds to prevent bonds between peptides. 4 mM of the peptide FGGC, synthesised by The Department of Molecules and Materials at the University of Twente (Enschede, The Netherlands), was dissolved in the TCEP solution. Thereafter, 2 mM of CB[8] (cucurbit[8]uril)(Sigma-Aldrich, St. Louis, MO, USA) was dissolved in this FGGC solution (2:1 FGGC:CB[8]) and placed in a sonificator (37 °C, 10 min)(HBM, Darmstadt, Germany) to increase the solubility.

Hydrogel precursor solutions were prepared following the conditions in Table 1. Each hydrogel contains 40 μL of 2% (w/v) ALGAEMA(-RGD) solution and every condition is executed in triplets. In conditions A and B, the 4% (w/v) ALGAEMA and the 4% ALGAEMA-RGD were diluted to 2% (w/v) ALGAEAM-(RGD) with Milli-Q. For conditions C and D, the 4% (w/v) ALGAEMA and 4% (w/v) ALGAEMA-RGD is diluted with the solution containing FGGC:CB[8] complex. 40μL of each hydrogel precursor solution was transferred to a 5 mm diameter Ecoflex mould. Initial experiments were conducted by encapsulating C2C12 cells and hiPSC-CMs. This is done by inserting the cells in the precursor solution before transferring the precursor to the mould and crosslinking the hydrogel. A more detailed protocol of this method is written in Section A.1 and Section A.2 in the Appendix.

Table 1: Different conditions of the prepared ALGAEMA hydrogel for cell culture.

Component	A	B	C	D
ALGAEMA	1	0	1	0
ALGAEMA-RGD	0	1	0	1
FGGC	0	0	1	1
CB[8]	0	0	1	1

3.2.1 Ecoflex mould

The mould used for the synthesis of the hydrogels is a flexible rubbery mould containing circular cavities. Three different positive moulds were designed in Solidworks® and 3D-printed. The first positive mould contains a pattern on the surface and has a total diameter of 5 mm and a height of 2 mm. The technical drawing of the patterns is shown in Figure 8. Pattern B contains grooves of 0,40 mm with a space of 0,20 mm in between. Pattern D contains grooves of 0,50 mm with a space of 0,10 mm in between. The height of both patterns is 0,20 mm. The second positive mould also has a diameter of 5 mm and a height of 2 mm and contains a rim of 0,1 mm. The third positive mould will be used for the rheology analysis and has diameters of 8 mm with a height of 2 mm.

In the positive 3D-printed moulds, Ecoflex™ 00-30 was poured to obtain a negative mould for the hydrogels. This is done following the manufacturer's guidelines and letting the mould cure overnight. Following this time, the negative Ecoflex moulds were extracted from the positive 3D-printed mould and kept at room temperature. The moulds meant for the cell culture were kept in a sterile environment.

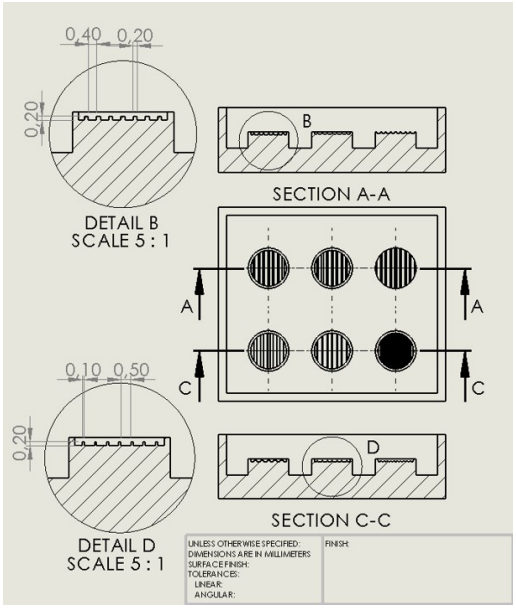

Figure 8: Technical drawing in Solidworks® of the positive mould highlighting patterns B and D for cell culture. The poured and cured Ecoflex™ 00-30 mould will be extracted from the 3D-printed mould and employed as the inverse mould for the hydrogels produced within it.

3.2.2 UV-crosslinking

When the functionalised ALGAEMA is transferred to the Ecoflex mould, the polymers will be covalently crosslinked by exposure to UV (ultraviolet). The radiation in combination with the photo-initiator LAP allows this UV-induced crosslinking. The casting and curing are done by a UV light setup containing a UV LED of 405 nm for 10 minutes (radiation dose = 10mW/cm^2, Volt = 3.88, Ampère = 2,55).

3.3 Rheology

For the assessment of the mechanical properties of the hydrogel, the measurements were conducted using the Rheometer Discovery HR 10 (TA instruments, inc, New Castle, DE, US) with a cross-hatched Peltier plate (TA Instruments, inc, New Castle, DE, US). In a non-sterile condition, 100µL hydrogels with the conditions following Table 2 were prepared in triplets and cast and cured in the mould meant for rheology. The hydrogels were swelled in PBS overnight before starting the rheology analysis.

Table 2: Different conditions of the prepared ALGAEMA hydrogel for rheology.

Component	A	B	C	D	E	F
ALGAEMA	1	0	0	1	1	0
ALGAEMA-RGD	0	1	1	0	0	1
FGGC	0	0	1	1	1	1
CB[8]	0	0	0	0	1	1

On every hydrogel, two measurements were conducted. First the time sweep (frequency 0,1 Hz and strain 1%) for determination of the storage modulus (G') and the loss modulus (G"). The second rheology measurement is the stress relaxation test. The same sample used for the time sweep is now exposed to a constant strain of 10% to measure the decrease in stress and the characteristic relaxation time.

3.4 Seeding cells

The hydrogels, created from 40 µL solution and crosslinked with UV in the Ecoflex mould were kept in a 96-well plate with 200μ L CM-DMEM (Provided by The Applied Stem Cell Technologies (AST) group of the University of Twente (Enschede, The Netherlands)). For positive control, three wells were filled with 100 μ L vitronectin (diluted in PBS 1:99), which is a glycoprotein present in the ECM. After 1h of incubation, 200 μ L of DMEM was added to wash the vitronectin-containing wells and removed after 30 min to seed the cells. As a second positive control, three wells were coated with Matrigel, a commercially available matrix derived from the Engelbreth–Holm–Swarm mouse tumor, which is rich in laminin, collagen and other ECM proteins [46]. For the coating of the wells with Matrigel, pre-cooled tips, pipettes, tubes and medium was used and the Matrigel Matrix aliquot was kept on ice all the time. The Matrigel Matrix was diluted 1:100 in DMEM complete and 0,05 ml/well was added to the 96-wellplate. The coated wells were incubated at room temperature and after 1h the Matrigel solution is aspirated and discarded.

3.4.1 Cell preparation hiPSC-CM's

The human induced pluripotent stem cell cardiomyocytes (hiPSC-CM's), provided by the Applied Stem Cell Technologies (AST) group of the University of Twente (Enschede, the Netherlands) were kept in liquid nitrogen (-197 °C) and transferred in ice when used. After thawing the cells in hot water (37 °C) the cells were transferred to a 15 mL tube from the cryo-vial. With the same tip, 1000 μL of CM-DMEM was used to wash the cryo-vial and the same medium was added drop by drop to the 15 mL tube with cells, with shaking between the drops. 4mL of DMEM was added drop by drop to the 15 mL tube and centrifuged for 3 min at 1100 rpm. The supernatant was removed and the remaining pellet was resuspended in 1000 μL CM-DMEM. After cell counting using a trypan blue staining and the Bürker-Türk counting chamber, the cells were diluted with CM DMEM to achieve 7,2 * 10^5 cells/hydrogel. In each condition, 200 μL of the cell suspension was added on top of the hydrogel and placed in the incubator (37 °C). Initially, after 24 h, 100 μL of DMEM complete was removed and new was added, and then after every 48 h.

3.5 Analysis of the cells

3.5.1 Alamar blue assay

The viability of the cells where analysed with an Alamar blue assay. For preparing the hydrogels for this assay, 200 μL of Alamar Blue Stain 0,4% (NanoEntek, South-Korea)(diluted 1:10 in DMEM complete) including the colour reagent resazurin (7-hydroxy-3H-phenaixazine-3-one-10-oxide) was added to each hydrogel in the 48-well plate and incubated for 2 h at 37 °C, packed in aluminium foil. The Alamar Blue stain in DMEM was added in empty wells to use as background control.

When Alamar Blue is added to hydrogels, resazurin will be converted by the cells into fluorescent resorufin (7-hydroxy-3H-phanoxazine). After incubation, 100 μL of each hydrogel-containing well was transferred to

a black 96-well microtiter plate and placed in The Enspire® Multimode Plate Reader (PerkinElmer, Waltham, MA, USA) for analysis.

3.5.2 Immunostaining

After transferring the hydrogel to a new 96-well plate, the hydrogels were washed with 100 μL DPBS 2 times for 5 min. 4% (w/v) PFA (perfluoroalkoxy alkane) was added and incubated for 10 min. Again the hydrogels were washed with DPBS 2 times for 5 min. Next, the samples were permeabilized with 100μL 0.3% (v/v) TritonX (10% diluted in PBS)(2-[4-(2,4,4-trimethylpentan-2-yl)phenoxy]ethanol) for 10 min. Then 100 μL of Blocking Buffer (BB) was added (0,1% (v/v) TritonX and 5% (v/v) BSA (Bovine serum albumin)) and left for 20 min. After the blocking, the samples were incubated with 100 μL Anti-Vinculin antibody (primary) V9264 (diluted in 1:200 BB) for 1h. After this 1h the samples were incubated with Alexa fluor anti-mouse 488 secondary antibody (diluted in 1:400 BB) and Phalloidin 647 (diluted in 1:100 BB) and washed after 1h with PBS for again 1h. The samples were washed with PBS two times for 5 min and incubated with DAPI (diluted in 1:1000 PBS) for 10 min. The analysis of the stained hydrogels has been done with the Zeiss LSM 880 confocal laser scanning microscope (Carl Zeiss AG, Oberkochen, Germany). The laser lines with wavelengths of 405 nm (DAPI), 488 nm (Alexa Fluor) and 633 nm (Phalloidin) with emission wavelengths of 470 nm, 525 nm and 668 nm, respectively were used for analysis. For these trials, a 10x objective and a 20x objective were used.

4 Results

4.1 Mechanical properties

The mechanical properties of the hydrogels have been determined using a rheology experiment, consisting of a time sweep and a stress relaxation test. The results of the time sweep, where the storage modulus (G'), and loss modulus (G") were determined, are presented in Figure 9 and the exact values together with the ratio of the loss tangent over the storage tangent in percentages (loss tangent) are presented in Table 3. The data is processed using the MATLAB script in the Appendix Chapter A.6.

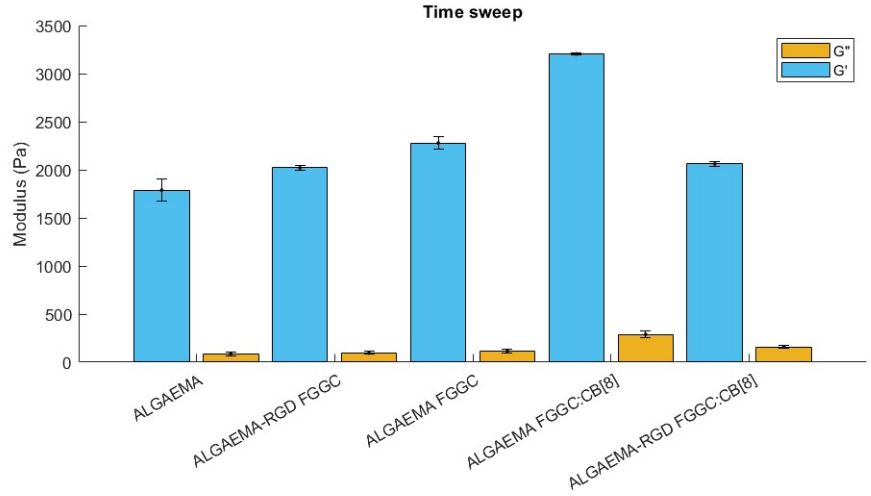

Figure 9: Timesweep of hydrogels with the storage modulus (G') and the loss modulus (G") of different concentrations described in Table 2.

The ALGAEMA FGGC:CB[8] hydrogel, shows the highest value for either G' and G", with a value of 3203 Pa and 289.38 Pa respectively. Conditions A with the ALGAEMA presents the lowest value of all the conditions with G' = 1789 Pa and G" = 87.88 Pa. The conditions containing the dynamic bonds exhibit the highest ratio of the loss modulus over the storage modulus.

Table 3: The exact values of the storage modulus (G'), the loss modulus (G") and the loss modulus over the storage modulus, known as the loss tangent, for the different conditions of the hydrogel.

Condition	**Storage modulus (G') [Pa]**	**Loss modulus (G") [Pa]**	**Loss tangent [%]**
ALGAEMA	1789	87.88	4.91%
ALGAEMA-RGD	2020	95.65	4.73%
ALGAEMA FGGC	2279	115.97	5.08%
ALGAEMA FGGC:CB[8]	3203	289.38	9.03%
ALGAEMA-RGD FGGC:CB[8]	2063	158.99	7.70%

The course of the stress dissipation and the corresponding half relaxation time (τ=1/2) is presented in Figure 10. The data is processed using the MATLAB script in the Appendix Chapter A.7. The blue line represents the condition containing ALGAEMA with τ= 866s. The orange line is the condition with ALGAEMA-RGD and τ= 864s. The yellow line contains the condition with ALGAEMA and FGGC with τ= 74s. The hydrogel with ALGAEMA and the FGGC:CB[8] complex is shown as the purple line with a τ = 41s and the green line represents the condition containing ALGAEMA-RGD and the FGGC:CB[8] complex with a τ =75s. The blue and the orange line exhibit approximately a similar trend, both demonstrating a τ=1/2 within the same segment. The yellow line also displays a similar trend but presents a much lower half relaxation time compared to the blue and orange line. The half relaxation time of the condition with ALGAEMA FGGC is nearly as low as the conditions with the FGGC:CB[8] complexes.

a)

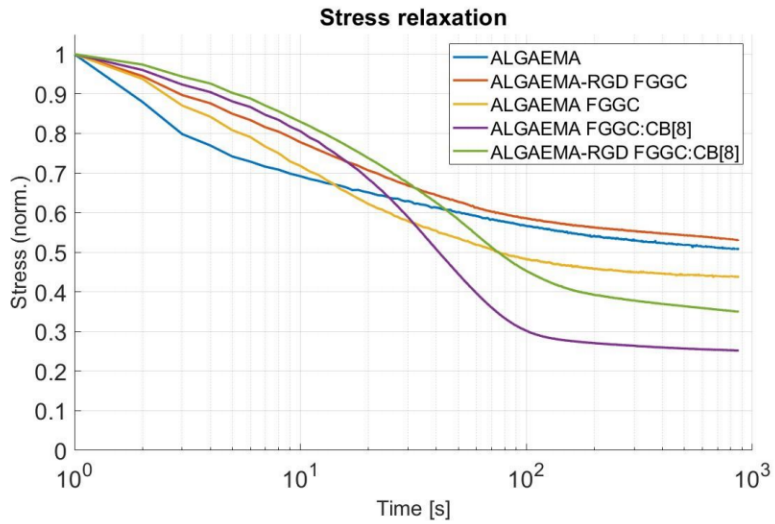

b)

Condition	τ [s]
ALGAEMA	866
ALGAEMA-RGD FGGC	864
ALGAEMA FGGC	74
ALGAEMA FGGC:CB[8]	41
ALGAEMA-RGD FGGC:CB[8]	75

Figure 10: Outcomes of stress relaxation measurements. a) Graph showing the progression of the decreasing stress in the different hydrogels under a constant strain of 10%. b) The half relaxation time $\tau = 1/2$ of the different conditions.

Figure 11 shows the result of the Youngs modulus using Formula 1 for each condition. The data is processed using the MATLAB script in the Appendix Chapter A.8. Condition D exhibits the highest Young's modulus and Condition A the lowest value for the Youngs modulus.

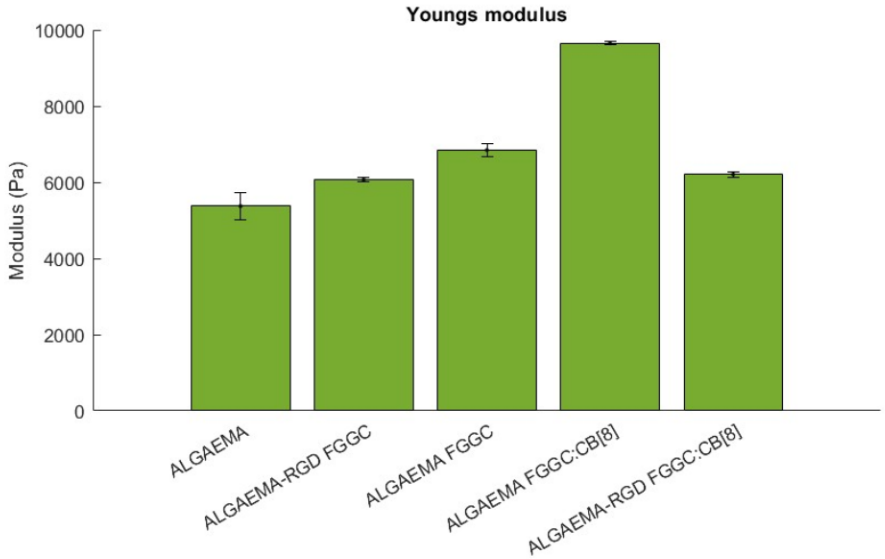

Figure 11: Bar graph of the Youngs modulus of the different conditions of the hydrogel.

4.2 Cell experiments

The behaviour of the cells in response to the different hydrogel compositions and surface roughnesses has been delineated through diverse cell experiments.

4.2.1 Cell morphology

Figure 12 shows the brightfield images of the encapsulated C2C12 cells on day 1 and day 8. The day after the encapsulation, the cells seem uniformly distributed through the hydrogel and contain the round shape form. Figure 12C with the RGD sequence included illustrates already some spreaded cells located on the surface of the hydrogel. The conditions that contain the FGGC:CB[8] complex (Figure 12D and E) are a bit turbid and it is hard to see the cells through the hydrogel. At day 8, the microscopic pictures of the encapsulated C2C12 cells in the conditions without the cell binding sequence RGD are still round-shaped. Figure 12H and J show the conditions with ALGAEMA-RGD and these conditions exhibit a high density of stretched cells on the surface. In Figure 12J, this has even developed into a highly dense complex of stretched cells.

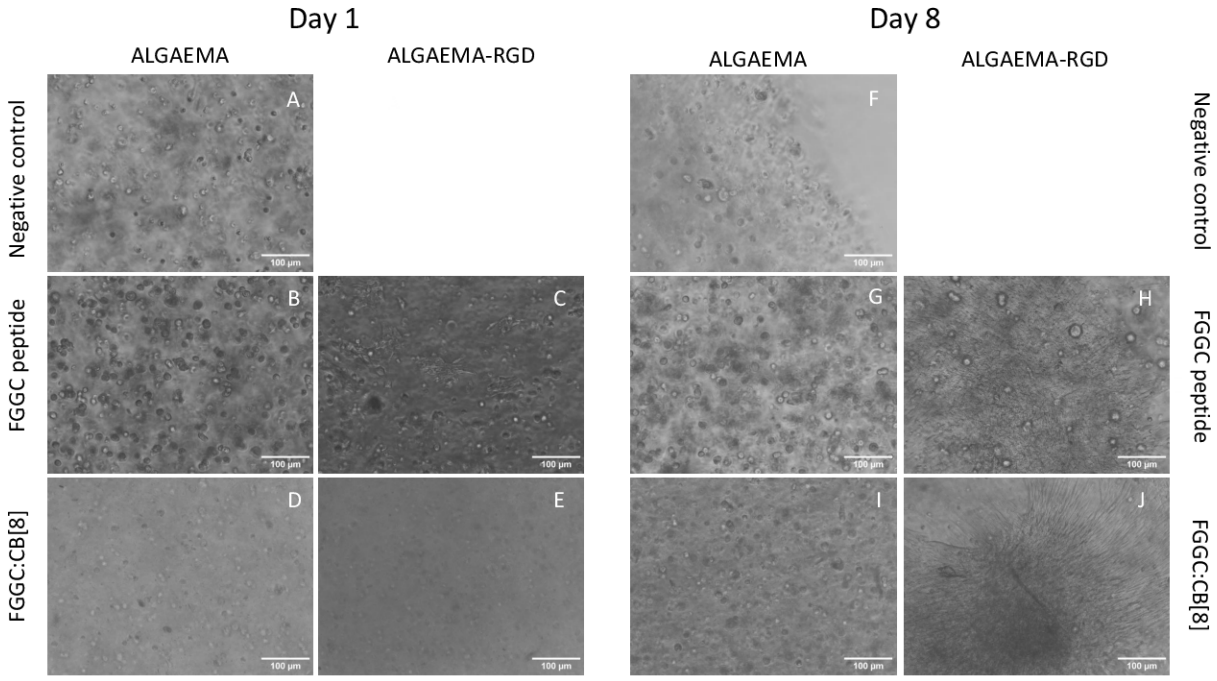

Figure 12: Brightfield microscopic images of encapsulated C2C12 cells in the hydrogel with different compositions. The pictures were taken the day after seeding (day 1) and on day 8.

The brightfield images on day 1 and day 3 of the encapsulated hiPSC-CMs are shown in Figure 13. The cells within the hydrogels acting as the negative control (Figure 13, first row) exhibit round-shaped hiPSC-CMs equally distributed within the hydrogel. During the experiment, cells leaked out of the hydrogel and primarily migrated to the bottom of the wellplate. Resulting in a lower density of hiPSC-CMs cells after every medium change and transfer of the hydrogel to a new well plate. After the preparation of the hydrogels containing CB[8], large fiber complexes are present within the hydrogel (Figure 13, bottom two rows). On day 3, there were still no spread and stretched cells detected. Neither in the hydrogel nor at the surface.

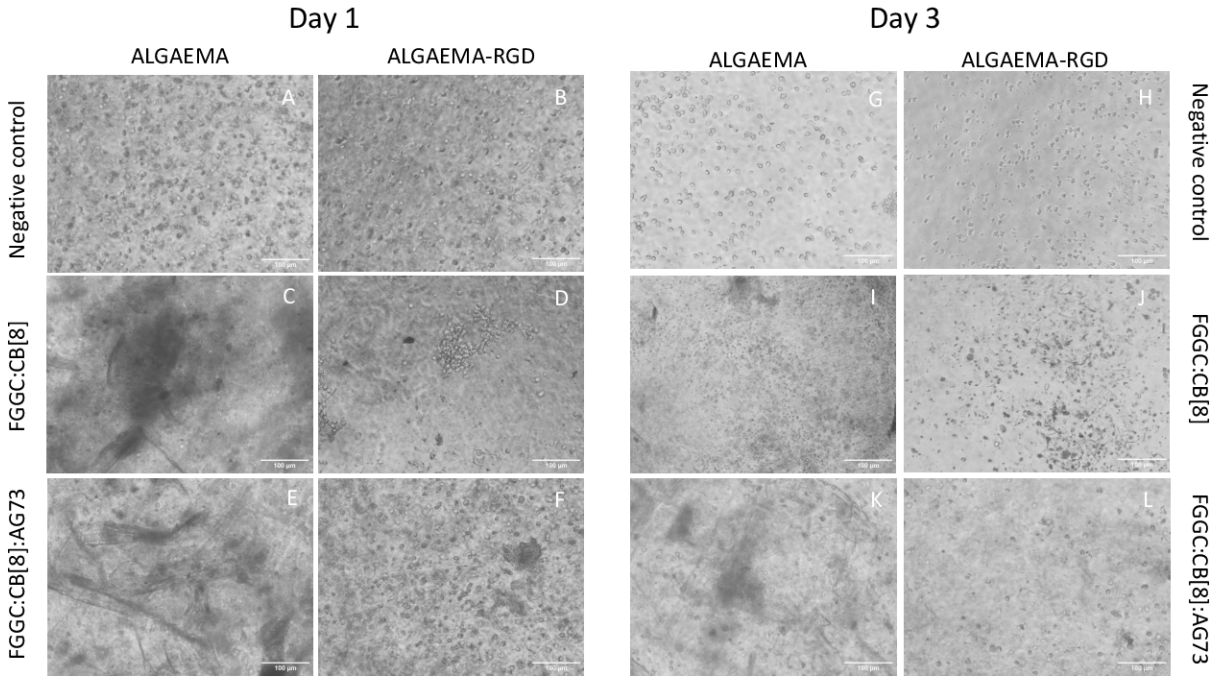

Figure 13: Brightfield microscopic images of encapsulated hiPSC-CMs in the hydrogel with different compositions. The pictures were taken the day after seeding (day 1) and at day 3.

The brightfield images of the hiPSC-CMs seeded on the surface of the hydrogel with and without a pattern (Figure 8 on day 1 are shown in Figure 14. On the surface of the hydrogel without a pattern and the FGGC:CB[8] complex (Figure 14A, B, G and H) the hiPSC-CMs are homogeneously distributed over the surface of the hydrogel and form round-shaped cells. An increased cell concentration has been observed at the bottom of the well plate adjacent to the hydrogel. The patterned hydrogels in Figure 14 (bottom two rows) result in a discernible alignment of cells with the varying groove sizes between pattern B and pattern D. In the conditions with dynamic bonds, this alignment is somewhat less pronounced but still present. Residual patterns were observed, but the majority of the cellular alignment on the alginate patterns was lost on days 3 and 5 (Figure 21 and 22, Appendix A.5), presumably due to the removal of cells during washing.

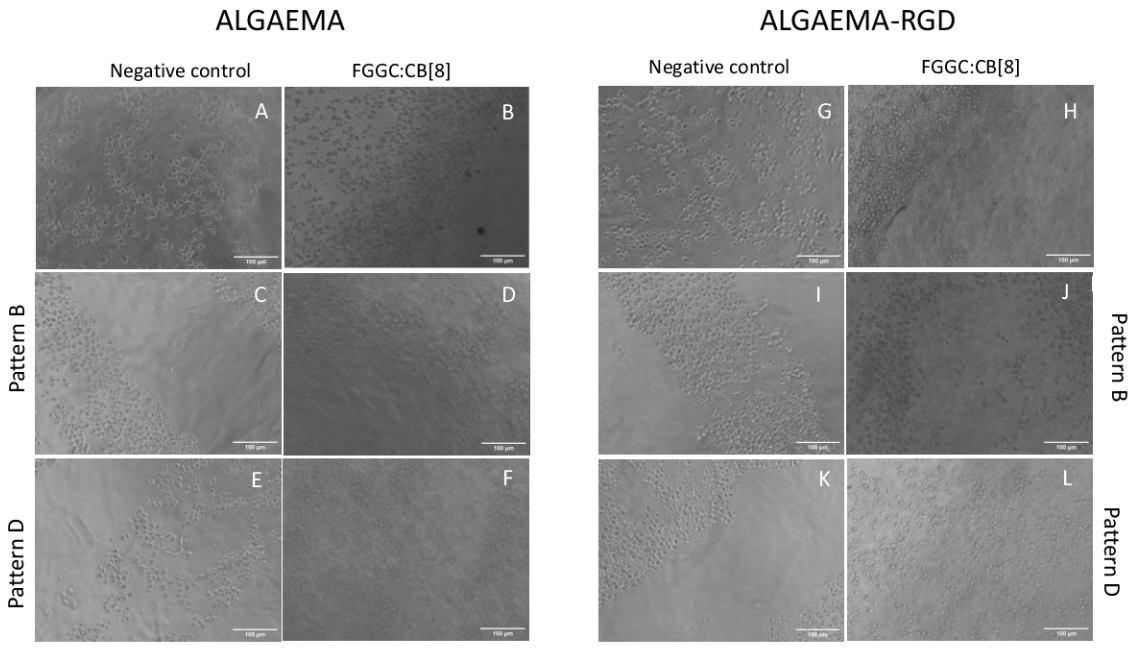

Figure 14: Brightfield images of the hiPSC-CMs seeded on the surface of the hydrogel at day 1. The images differ in terms of the composition of the hydrogel and the presence of a pattern on the surface. Pattern B contains grooves of 0,40 mm with a space of 0,20 mm between and pattern D contains 0,50 mm grooves with a space of 0,10 mm between (Figure 8).

4.2.2 Cell viability

The viability of the cells is measured using an Alamar Blue assay. The intensities of the different conditions are all relative to each other and are the result after subtracting the intensity of the background control measurement. The results of the experiments where the C2C12 cells and the hiPSC-CMs were encapsulated are shown in Figure 15. The first graph (Figure 15a) represents the cell viability of the encapsulated C2C12 cells after day 1 in the hydrogel conditions following Table 4. The second graph (Figure 15b) contains the cell viability measurements of the encapsulated hiPSC-CMs after day 1 in the hydrogel conditions according to Table 5. All the conditions of Figure 15B showed negative values for the intensity which indicates that there were fewer signals detected than in the background control well.

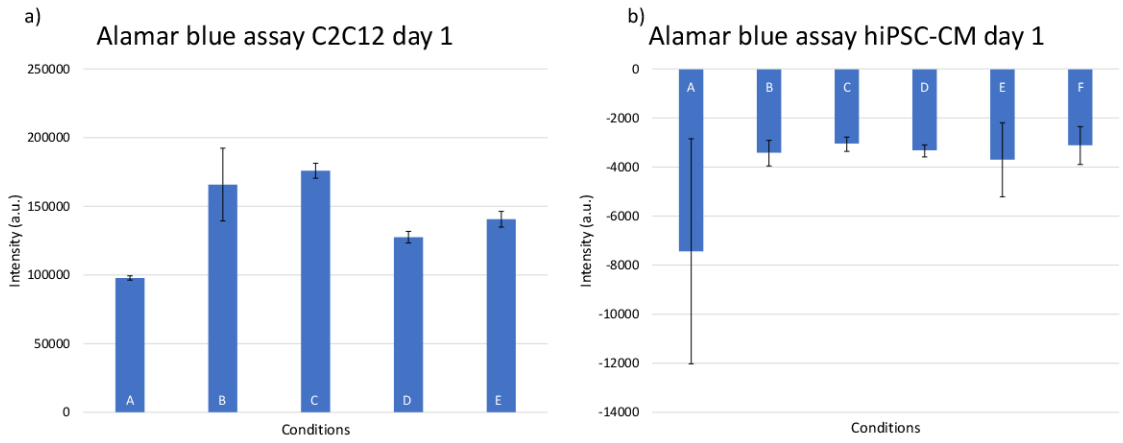

Figure 15: Results of the Alamar Blue assay. a) Cell viability of the encapsulated C2C12 cells at day 1. b) Cell viability of the encapsulated hiPSC-CMs at day 1.

The cell viability results of the surface seeding experiments with hiPSC-CMs on the hydrogel conditions according to Table 1 at day 8 are shown in Figure 16. Also here the indicates the negative values for the intensity, that there were fewer signals detected than in the background control well. The well that serves as a positive control (PC) contained the Matrigel coating and showed negative values for the viability of the cells as well.

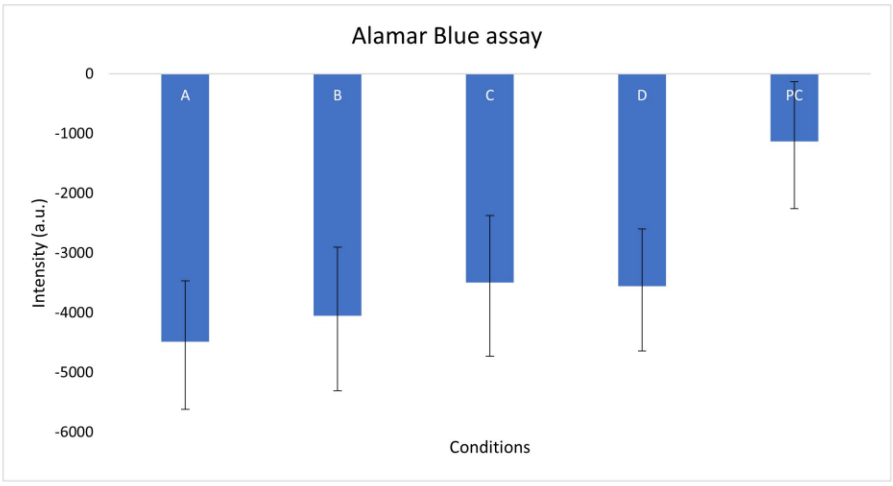

Figure 16: Results of the Alamar Blue assay executed 8 days after seeding the hiPSC-CMs on the surface of the hydrogels.

4.2.3 Cell adhesion

By staining the protein vinculin, the cytoskeleton actin and the DNA in the cell nucleus, cell adhesion is visualized. In Figure 17, the images of the stained C2C12 cells after 17 days in the ALGAEAMA-(RGD) are shown.

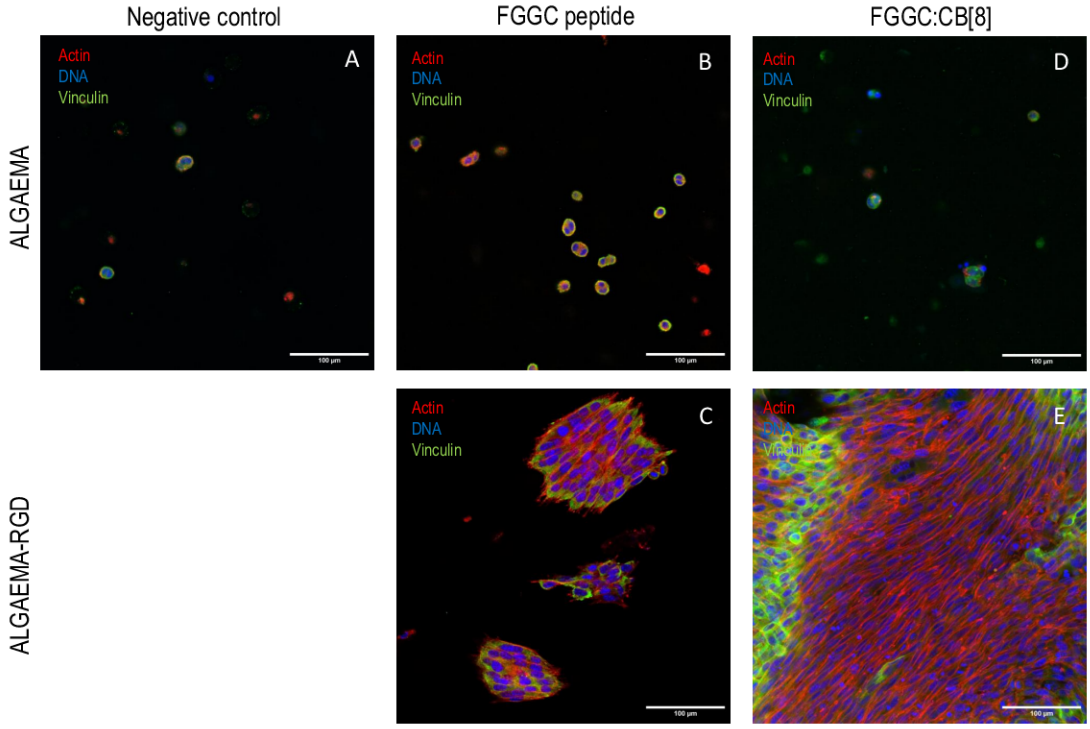

Figure 17: Confocal images of the C2C12 cells encapsulated in the hydrogel. The pictures are taken with the Zeiss LSM 880 confocal laser scanning microscope and a 20x objective. The actin is stained with Phalloidin 647 in red, the DNA with DAPI in blue and the protein vinculin with Alexa fluor in green.

The conditions without C-RGD (Figure 17A, B and D) do not show any spreading or attachment. The stained nucleus and cell membrane remain round-shaped and no spreading or attachment can be detected. The conditions including C-RGD (Figure 17C and E) show a high confluence in cell adhesion and spreading. The actin filaments are stretched and the bright red and green dots on the surface of the cells represent FACs. The stretched cells in Figure 17C are more clustered and less abundant than the cells in Figure 17E, where there is a high confluency of stretched cells. In both conditions, the protein vinculin is mainly localized at the end of the stretched actin filaments where the FAC complexes are formed.

5 Discussion

5.1 Mechanical properties

In addition to the presence of double bonds, the bindings of FGGC and C-RGD can also contribute to increased viscoelastic properties of the hydrogel. Both FGGC and C-RGD bind through the cysteine side group with the double bonds of AEMA, leading to a reduced number of available double bonds for the covalent crosslinking of the hydrogel. However, the concentration of C-RGD is 282 μM per hydrogel, while the concentration of FGGC is 2 mM. This suggests that the contribution of C-RGD is negligible compared to FGGC. Nevertheless, the presence of FGGC does not seem to reflect in the mechanical properties between hydrogels containing and not containing FGGC.

In Figure 9 the values of the storage modulus (G') and the loss modulus (G") are shown. Since the storage modulus (G') represents the stored energy in an elastic hydrogel and the loss modulus the dissipated energy [42], the ratio of the loss modulus over the storage modulus indicates the viscoelastic properties of the hydrogel. The hydrogels with dynamic bonds exhibit a higher loss tangent. This aligns with the expectation that dynamic bonds should result in more viscoelastic properties. However, the storage modulus increases when using dynamic bonds, when compared with the hydrogels with ALGAEMA-(RGD) and FGGC, where only covalent crosslinks are present. Although the conditions with FGGC:CB[8], exhibit a higher storage modulus than the conditions without dynamic bonds (Table 3), the loss modulus increases as well.

For the stress relaxation measurements, the hydrogels without the dynamic bonds show little stress relaxation with a higher half relaxation time. Except for the condition with ALGAEMA FGGC (yellow line in Figure 10). Figure 19 in Appendix A.3, reveals that one of the hydrogels with ALGAEMA FGGC contains a half relaxation time of 861s, which is closer to the half relaxation time of the hydrogels without the dynamic bonds. The other two hydrogels of ALGAEMA FGGC exhibit a lower half relaxation time which decreases the mean of the three half relaxation times. However, the half relaxation time of D is considerably lower than that of E. Differences or outliers in the sample preparations might explain the deviation in both the trend line and the half relaxation time values compared to the other data points including dynamic bonds. Furthermore, the conditions including the FGGC:CB[8] complexes show a similar stress dissipation trend.

The results of the Youngs modulus are considerably higher compared to those reported in the literature. Engler et al. (2008) studied that the Youngs modulus (E) of the embryonic myocardium is in the range of 2-4 kPa [23]. Wheelwright et al. examined that the hiPSC-CMs produce significantly more force on a substrate with a modulus of 3.1 kPa than on a 9.8 or 13.5 kPa modulus substrate [25] and Alonzo et. al describe that the optimal E for an alginate-based hydrogel that resembles embryonic cardiac tissue is 2.66 ± 0,84 kPa and for normal cardiac tissue 8.98 ± 3.17 kPa [47]. All these study shows that the results of E of the alginate-based hydrogel containing the dynamic bonds, are more close to the elastic modulus of that of adult ECM and thus too high to mimic the embryonic ECM. Utilization of alternative dynamic bonds might offer a solution to approximate the viscoelastic properties of the embryonic ECM. In the study of Rowland et al. the crosslinking method consists only of the dynamic bonds, which serve as linkers for the alginate strands. So the hydrogel is formed solely through the interaction of FGGC and CB[8] with the AEMA [48]. Additionally, a method involving the addition of a cysteine group to the opposite end of the C-RGD sequence, resulting in the peptide sequence that can act as a linker between the polymer strands. Factors that could be further adjusted in the current protocol to obtain a more viscoelastic material include decreasing the photo-initiator concentration, which results in a reduced generation of free radicals responsible for covalently crosslinking the hydrogel.

5.2 Cell behaviour

The initial experiments involving the encapsulation of the C2C12 cells demonstrated that the cells mainly spread and attach on the surface. The C2C12 cells survived the presence of the photo-initiator and the UV radiation when preparing the hydrogel, enabling attachment and spreading of the cells. The immunostaining and microscopic images do reveal that the attachment and spreading exclusively occur on the surface of the hydrogel containing C-RGD, where there is more space available. The presence of this cell-binding peptide sequence is thus necessary for enabling C2C12 to spread and attach. Also the higher confluence in the hydrogel

with C-RGD and the FGGC:CB[8] complex indicates the ability of the C2C12 to break the dynamic bonds to create a greater surface where C-RGD is exposed to and creates space within the matrix to allow C2C12 cells to migrate. For further steps, the staining of the C-RGD peptide sequences could be an interesting method to map the distribution, given the strong dependency of cell attachment on their presence.

The experiments involving the encapsulation of the hiPSC-CMs demonstrated, based on both cell viability assessments and the microscopic images, a diminished count of viable cells. The presence of the photo-initiator and the UV-radiation could be the explanatory factor since covalent crosslinking reactions may induce toxicity to the sensitive hiPSC-CMs. [33]. A positive control with a fibrin hydrogel (Section A.4 in the Appendix) demonstrated a high viability with even an observed contractile force after a few days. This highlighted the need to delete the cells from the covalent crosslinking process and seed the cells on the surface after crosslinking. This approach was anticipated to increase the chances of cell survival and enable the hiPSC-CMs to adhere and spread on the surface providing the ability to still investigate the influence of the viscoelastic properties and the surface roughness on the behaviour of the cells. The dynamic bonds would still contribute to the reduced stiffness of the hydrogel for the cells to contract against and act as breakable bonds by the cells, allowing more space for the cells to bind to the C-RGD. The conditions consisting of ALGAEMA lacked sites for cell binding, hence reducing the likelihood of cell attachment and binding. Therefore, these conditions were solely intended for control purposes. However, this new approach also led to a low viability of the hiPSC-CMs. This was confirmed through the microscopic images and an Alamar Blue assay (Figure 13). The explanation for this can be the low availability of the C-RGD peptide sequence on the surface, which results in the inability of the cells to attach to the hydrogel. During the ALGAEMA-RGD preparation, 282 μM of C-RGD was added to the ALGAEMA, which was lower than initially determined. Utilizing higher concentrations in the range of mM of C-RGD instead of μM, leads to a higher probability of attaching the cells to the C-RGD sequence and hypothetically to improved results.

The patterns on the surface of the hydrogel facilitate a proper alignment of cells within the grooves as was observed on day 1. However, throughout the experiment, this alignment gradually diminishes. This could be attributed to the medium changes every 48h. Since it is observed that the cells are not strongly attached to the surface, they may be lost or displaced during the medium change due to the pressure from pipetting.

In addition to the requirement for cells to have cell-matrix interactions for survival, cell-cell interactions are also essential. The cell-matrix interactions are observed through microscopic and stained images, showing the change in cell morphology from a rounded, unattached sphere to an elongated and stretched cell. Immunostaining allows the analysis of the cell-matrix interaction by staining the cytoskeleton and proteins like vinculin. However, cell-cell interactions cannot be observed directly through the microscope but rather after staining the junctions. As the cells exhibited minimal signs of viability and the Alamar Blue assays were not very positive, eventually, no immunostaining was conducted on the hiPSC-CMs since both interactions are crucial for cell survival.

The primary issue concerning the validity of the study with the cultured cells is that the positive control also shows no observable attachment and spreading, along with negative cell viability. Consequently, concluding differences among the hydrogel composites is challenging due to the cells' inability to survive under any condition. To address this, the coating of the positive control was altered from vitronectin to Matrigel to eliminate any potential dysfunction associated with vitronectin. However, even in the presence of this alternative coating, the cells still perished. Possible reasons for this could further relate to the utilization of the specific cell culture-well plate or maintaining more consistency in cooling the cells between actions. Subsequent research should therefore initially investigate these factors to enhance cell viability and identify differences in viability among the conditions.

6 Conclusion and Outlook

The objective of this study is to investigate the influence of the viscoelastic properties and surface roughnesses of an alginate-based hydrogel on the behaviour of hiPSC-CMs. Through the low viability of the positive control, no conclusion can be drawn on this particular situation regarding the behaviour of the cells.

However, several other aspects of the behaviour of the cells and the mechanical properties of the hydrogel can be concluded. The method of covalently crosslinking with the specific concentration of photo-initiator and UV-radiation harms the cells resulting in cell death. A different and cytocompatible approach to crosslinking is desired. For example, crosslinking with the host-guest complex FGGC:CB[8], since the cysteine of both peptides can bind to the AEMA, or the addition of a cysteine group to the opposite end of a C-RGD sequence.

The applied surface roughnesses do facilitate cell alignment in the grooves of both patterns, but little can be inferred about long-term behaviour of the hiPSC-CMs, as both patterned and non-patterned hydrogels exhibited no adhesion and experienced cell death. As a result of refreshing the medium, the cells were washed away, which would not occur if the cells were attached. Further research could state whether increasing the perimeter indeed has an effect and thereby enhances the concentration of C-RGD on the surface. This can be validated through staining of the C-RGD peptide sequence.

The presence of the FGGC:CB[8] complexes within the hydrogel leads to a higher percentage of the loss tangent, a lower half relaxation time, and exhibit stress relaxation. All of these factors are associated with a more viscoelastic material. However, the values of the Youngs modulus (E) are not yet close to those of embryonic tissue [25][23][47], so multiple adjustments must be made to achieve this viscoelasticity.

Further research should initially focus on the treatment of the hiPSC-CMs. The reason for the low viability despite favourable coating, is important to continue regarding the cell culture experiments. Only then can actual conclusions be made regarding the presence of surface roughness and the dynamic bonds within the hydrogel.

7 Acknowledgements

First of all, I want to thank Nataliya Debera for her extending patience and time in guiding me during the project. Without her extensive feedback and daily assistance, I would not have been able to conduct the experiments and write this thesis. In particular, my increased chemical calculation skills, as a result of her comprehensive and patient explanations.

I also would like to thank Prof. dr. ir. Pascal Jonkheijm, for giving me the opportunity to do my bachelor thesis in the Molecular Nanofabrication Faculty and for the positive feedback and thoughtful contributions during the meetings. I further want to thank Prof. dr. Robert C.J.J Passier for being the external committee member in this bachelor thesis.

Finally, I would like to thank my friends and family for helping, enduring support and genuine interest in my project. Without this support, I would not have been able to finish this thesis.

Referenties

1. Wang Z, Lee SJ, Cheng HJ, Yoo JJ en Atala A. 3D bioprinted functional and contractile cardiac tissue constructs. Acta biomaterialia 2018 Apr; 70:48–56. DOI: 10.1016/J.ACTBIO.2018.02.007. Available from: https://pubmed.ncbi.nlm.nih.gov/29452273/
2. Patel L, Worch JC, Dove AP en Gehmlich K. The Utilisation of Hydrogels for iPSC-Cardiomyocyte Research. International Journal of Molecular Sciences 2023; 24:9995. DOI: 10.3390/ijms24129995
3. Zhang Y, Wang Z, Sun Q, Li Q, Li S en Li X. Dynamic Hydrogels with Viscoelasticity and Tunable Stiffness for the Regulation of Cell Behavior and Fate. Materials 2023 Jul; 16. DOI: 10.3390/MA16145161. Available from: /pmc/articles/PMC10386333/%20/pmc/articles/PMC10386333/?report=abstract%20https://www.ncbi.nlm.nih.gov/pmc/articles/PMC10386333/
4. Chaudhuri O. Viscoelastic hydrogels for 3D cell culture. Biomaterials science 2017 Aug; 5:1480–90. DOI: 10.1039/C7BM00261K. Available from: https://pubmed.ncbi.nlm.nih.gov/28584885/
5. Stowers RS. Advances in Extracellular Matrix-Mimetic Hydrogels to Guide Stem Cell Fate. Cells Tissues Organs 2022; 211:36–53. DOI: 10.1159/000514851
6. Tran DB, Weber C en Lopez RA. Anatomy, Thorax, Heart Muscles. StatPearls 2022 Dec. Available from: https://www.ncbi.nlm.nih.gov/books/NBK545195/
7. Gopalan C en Kirk E. The heart. Academic Press, 2022 Jan :1–33. DOI: 10.1016/B978-0-12-823421-1.00011-1. Available from: https://linkinghub.elsevier.com/retrieve/pii/B9780128234211000111
8. Marieb EN en Hoehn KN. Human Anatomy & Psysiology. Red. door Pearson Education. Deel 11. Pearson Education Limited, 2019 :1272
9. Jimenez-Vazquez EN, Jain A en Jones DK. Enhancing iPSC-CM Maturation Using a Matrigel-Coated Micropatterned PDMS Substrate. Current Protocols 2022 Nov; 2:e601. DOI: 10.1002/CPZ1.601. Available from: https://onlinelibrary.wiley.com/doi/full/10.1002/cpz1.601%20https://onlinelibrary.wiley.com/doi/abs/10.1002/cpz1.601%20https://currentprotocols.onlinelibrary.wiley.com/doi/10.1002/cpz1.601
10. Li J, Hua Y, Miyagawa S, Zhang J, Li L, Liu L en Sawa Y. hiPSC-Derived Cardiac Tissue for Disease Modeling and Drug Discovery. International Journal of Molecular Sciences 2020 Dec; 21:1–32. DOI: 10.3390/IJMS21238893. Available from: /pmc/articles/PMC7727666/%20/pmc/articles/PMC7727666/?report=abstract%20https://www.ncbi.nlm.nih.gov/pmc/articles/PMC7727666/
11. Schwach V en Passier R. Native cardiac environment and its impact on engineering cardiac tissue. Biomaterials Science 2019 Aug; 7:3566–80. DOI: 10.1039/C8BM01348A. Available from: https://pubs.rsc.org/en/content/articlehtml/2019/bm/c8bm01348a%20https://pubs.rsc.org/en/content/articlelanding/2019/bm/c8bm01348a
12. Ribeiro AJ, Ang YS, Fu JD, Rivas RN, Mohamed TM, Higgs GC, Srivastava D en Pruitt BL. Contractility of single cardiomyocytes differentiated from pluripotent stem cells depends on physiological shape and substrate stiffness. Proceedings of the National Academy of Sciences of the United States of America 2015 Sep; 112:12705–10. DOI: 10.1073/PNAS.1508073112. Available from: https://europepmc.org/articles/PMC4611612%20https://europepmc.org/article/MED/26417073
13. Liao H, Qi Y, Ye Y, Yue P, Zhang D en Li Y. Mechanotranduction Pathways in the Regulation of Mitochondrial Homeostasis in Cardiomyocytes. Frontiers in Cell and Developmental Biology 2021 Jan; 8:625089. DOI: 10.3389/FCELL.2020.625089/BIBTEX
14. Tracy RE en Sander GE. Histologically measured cardiomyocyte hypertrophy correlates with body height as strongly as with body mass index. Cardiology Research and Practice 2011; 1. DOI: 10.4061/2011/658958

15. Sheikh F, Ross RS en Chen J. Cell-Cell Connection to Cardiac Disease. Trends in Cardiovascular Medicine 2009; 19:182–90. DOI: 10.1016/j.tcm.2009.12.001. Available from: http://dx.doi.org/10.1016/j.tcm.2009.12.001

16. Yue B. NIH Public Access Author Manuscript J Glaucoma. Author manuscript; available in PMC 2015 October 01. Published in final edited form as: J Glaucoma. 2014 ; : S20–S23. doi:10.1097/IJG.0000000000000108. Biology of the Extracellular Matrix: An Overview Beatri. J Glaucoma. 2014; 23:1–7. DOI: 10.1097/IJG.0000000000000108.Biology. Available from: https://www.ncbi.nlm.nih.gov/pmc/articles/PMC3624763/pdf/nihms412728.pdf

17. What is the Extracellular Matrix? Available from: https://www.sigmaaldrich.com/NL/en/technical-documents/technical-article/cell-culture-and-cell-culture-analysis/3d-cell-culture/extracellular-matrix

18. Monte-Nieto G del, Fischer JW, Gorski DJ, Harvey RP en Kovacic JC. Basic Biology of Extracellular Matrix in the Cardiovascular System, Part 1/4: JACC Focus Seminar. Journal of the American College of Cardiology 2020 May; 75:2169. DOI: 10.1016/J.JACC.2020.03.024. Available from: /pmc/articles/PMC7324287/%20/pmc/articles/PMC7324287/?report=abstract%20https://www.ncbi.nlm.nih.gov/pmc/articles/PMC7324287/

19. Frantz C, Stewart KM en Weaver VM. The extracellular matrix at a glance. Journal of Cell Science 2010 Dec; 123:4195. DOI: 10.1242/JCS.023820. Available from: /pmc/articles/PMC2995612/%20https://www.ncbi.nlm.nih.gov/pmc/articles/PMC2995612/

20. Nielsen SH, Mouton AJ, DeLeon-Pennell KY, Genovese F, Karsdal M en Lindsey ML. Understanding Cardiac Extracellular Matrix Remodeling to Develop Biomarkers of Myocardial Infarction Outcomes. Matrix biology : journal of the International Society for Matrix Biology 2019 Jan; 75-76:43. DOI: 10.1016/J.MATBIO.2017.12.001. Available from: /pmc/articles/PMC6002886/%20/pmc/articles/PMC6002886/?report=abstract%20https://www.ncbi.nlm.nih.gov/pmc/articles/PMC6002886/

21. Chaudhuri O, Gu L, Darnell M, Klumpers D, Bencherif SA, Weaver JC, Huebsch N en Mooney DJ. Substrate stress relaxation regulates cell spreading. Nature communications 2015; 6:6364. DOI: 10.1038/NCOMMS7365. Available from: /pmc/articles/PMC4518451/%20/pmc/articles/PMC4518451/?report=abstract%20https://www.ncbi.nlm.nih.gov/pmc/articles/PMC4518451/

22. Chaudhuri O, Cooper-White J, Janmey PA, Mooney DJ en Shenoy VB. Effects of extracellular matrix viscoelasticity on cellular behaviour. Nature 2020; 584:535–46. DOI: 10.1038/s41586-020-2612-2. Available from: http://dx.doi.org/10.1038/s41586-020-2612-2

23. Engler AJ, Carag-Krieger C, Johnson CP, Raab M, Tang HY, Speicher DW, Sanger JW, Sanger JM en Discher DE. Embryonic cardiomyocytes beat best on a matrix with heart-like elasticity: scar-like rigidity inhibits beating. Journal of cell science 2008 Nov; 121:3794. DOI: 10.1242/JCS.029678. Available from: /pmc/articles/PMC2740334/%20/pmc/articles/PMC2740334/?report=abstract%20https://www.ncbi.nlm.nih.gov/pmc/articles/PMC2740334/

24. Wang Z, Golob MJ en Chesler NC. Viscoelastic Properties of Cardiovascular Tissues. Viscoelastic and Viscoplastic Materials 2016 Sep. DOI: 10.5772/64169. Available from: https://www.intechopen.com/chapters/51650

25. Wheelwright M, Win Z, Mikkila JL, Amen KY, Alford PW en Metzger JM. Investigation of human iPSC-derived cardiac myocyte functional maturation by single cell traction force microscopy. PLOS ONE 2018 Apr; 13:e0194909. DOI: 10.1371/JOURNAL.PONE.0194909. Available from: https://journals.plos.org/plosone/article?id=10.1371/journal.pone.0194909

26. Chaudhuri O, Gu L, Klumpers D, Darnell M, Bencherif SA, Weaver JC, Huebsch N, Lee HP, Lippens E, Duda GN en Mooney DJ. Hydrogels with tunable stress relaxation regulate stem cell fate and activity. Nature materials 2016 Mar; 15:326. DOI: 10.1038/NMAT4489. Available from: /pmc/articles/PMC4767627/%20/pmc/articles/PMC4767627/?report=abstract%20https://www.ncbi.nlm.nih.gov/pmc/articles/PMC4767627/

27. Schwartz MA. Integrins and extracellular matrix in mechanotransduction. Cold Spring Harbor perspectives in biology 2010; 2. DOI: 10.1101/CSHPERSPECT.A005066. Available from: https://pubmed.ncbi.nlm.nih.gov/21084386/

28. Israeli-Rosenberg S, Manso AM, Okada H en Ross RS. Integrins and Integrin-Associated Proteins in the Cardiac Myocyte. Circulation research 2014 Jan; 114:572. DOI: 10.1161/CIRCRESAHA.114.301275. Available from: /pmc/articles/PMC3975046/%20/pmc/articles/PMC3975046/?report=abstract%20https://www.ncbi.nlm.nih.gov/pmc/articles/PMC3975046/

29. Chaudhuri O, Cooper-White J, Janmey PA, Mooney DJ en Shenoy VB. The impact of extracellular matrix viscoelasticity on cellular behavior. Nature 2020 Aug; 584:535. DOI: 10.1038/S41586-020-2612-2. Available from: /pmc/articles/PMC7676152/%20/pmc/articles/PMC7676152/?report=abstract%20https://www.ncbi.nlm.nih.gov/pmc/articles/PMC7676152/

30. Liberski A, Latif N, Raynaud C, Bollensdorff C en Yacoub M. Alginate for cardiac regeneration: From seaweed to clinical trials. Global Cardiology Science & Practice 2016 Mar; 2016. DOI: 10.21542/GCSP.2016.4. Available from: /pmc/articles/PMC5642828/%20/pmc/articles/PMC5642828/?report=abstract%20https://www.ncbi.nlm.nih.gov/pmc/articles/PMC5642828/

31. Ahearne M, Yang Y, El Haj AJ, Then KY en Liu KK. Characterizing the viscoelastic properties of thin hydrogel-based constructs for tissue engineering applications. Journal of the Royal Society Interface 2005; 2:455–63. DOI: 10.1098/rsif.2005.0065

32. Ruvinov E en Cohen S. Alginate biomaterial for the treatment of myocardial infarction: Progress, translational strategies, and clinical outlook: From ocean algae to patient bedside. Advanced Drug Delivery Reviews 2016 Jan; 96:54–76. DOI: 10.1016/J.ADDR.2015.04.021

33. Lee KY en Mooney DJ. Alginate: Properties and biomedical applications. Progress in Polymer Science (Oxford) 2012; 37:106–26. DOI: 10.1016/j.progpolymsci.2011.06.003. Available from: http://dx.doi.org/10.1016/j.progpolymsci.2011.06.003

34. Li B, Li X, Chu X, Lou P, Yuan Y, Zhuge A, Zhu X, Shen Y, Pan J, Zhang L, Li L en Wu Z. Microecology restoration of colonic inflammation by in-Situ oral delivery of antibody-laden hydrogel microcapsules. Bioactive Materials 2022 Sep; 15:305–15. DOI: 10.1016/J.BIOACTMAT.2021.12.022

35. Jeon O, Bouhadir KH, Mansour JM en Alsberg E. Photocrosslinked alginate hydrogels with tunable biodegradation rates and mechanical properties. Biomaterials 2009 May; 30:2724–34. DOI: 10.1016/J.BIOMATERIALS.2009.01.034

36. Jia J, Coyle RC, Richards DJ, Lloyd C, Walker R, Biggs J, Chou CJ, Trusk TC en Mei Y. Acta Biomaterialia Development of peptide-functionalized synthetic hydrogel microarrays for stem cell and tissue engineering applications. Acta Biomaterialia 2016; 45:110–20. DOI: 10.1016/j.actbio.2016.09.006. Available from: http://dx.doi.org/10.1016/j.actbio.2016.09.006

37. Martinez-garcia FD, Hilster RHJ de, Sharma PK, Borghuis T, Hylkema MN, Burgess JK en Harmsen MC. Architecture and composition dictate viscoelastic properties of organ-derived extracellular matrix hydrogels. Polymers 2021; 13. DOI: 10.3390/polym13183113

38. Baby DK. Rheology of hydrogels. Rheology of Polymer Blends and Nanocomposites: Theory, Modelling and Applications 2020 Jan :193–204. DOI: 10.1016/B978-0-12-816957-5.00009-4

39. Basics of rheology — Anton Paar Wiki. Available from: https://wiki.anton-paar.com/en/basics-of-rheology/#viscoelastic-behavior

40. Lee D, Zhang H en Ryu S. Elastic Modulus Measurement of Hydrogels. *Cellulose-Based Superabsorbent Hydrogels*. Springer, Cham, 2018 :1–21. DOI: 10.1007/978-3-319-76573-0{_}60-1. Available from: https://link.springer.com/referenceworkentry/10.1007/978-3-319-76573-0_60-1

41. TA Instruments. Rheology. 2010 :20031

42. Viscoelasticity and dynamic mechanical testing A. Franck, TA Instruments Germany

43. Ashter SA. Characterization. Thermoforming of Single and Multilayer Laminates 2014 Jan :147–92. DOI: 10.1016/B978-1-4557-3172-5.00007-4. Available from: https://linkinghub.elsevier.com/retrieve/pii/B9781455731725000074

44. Wang M en Wang C. Bulk Properties of Biomaterials and Testing Techniques. Encyclopedia of Biomedical Engineering 2019 Jan; 1-3:53–64. DOI: 10.1016/B978-0-12-801238-3.99861-1

45. Wang Z, Shui M, Wyman IW, Zhang QW en Wang R. Cucurbit[8]uril-based supramolecular hydrogels for biomedical applications. RSC Medicinal Chemistry 2021; 12:722–9. DOI: 10.1039/d1md00019e

46. Conboy I, Freimer J, Weisenstein L, Liu Y, Mehdipour M en Gathwala R. 6.13 Tissue Engineering of Muscle Tissue. *Comprehensive Biomaterials II*. Elsevier, 2017 Jan :216–35. DOI: 10.1016/B978-0-12-803581-8.10178-X

47. Alonzo M, Kumar SA, Allen S, Delgado M, Fabian Alvarez-Primo ·, Suggs L en Binata Joddar ·. Hydrogel scaffolds with elasticity-mimicking embryonic substrates promote cardiac cellular network formation. Progress in Biomaterials 2020; 9:125–37. DOI: 10.1007/s40204-020-00137-0. Available from: https://doi.org/10.1007/s40204-020-00137-0

48. Rowland MJ, Appel EA, Coulston RJ en Scherman OA. Dynamically crosslinked materials via recognition of amino acids by cucurbit[8]uril. Journal of Materials Chemistry B 2013 May; 1:2904–10. DOI: 10.1039/C3TB20180E. Available from: https://pubs.rsc.org/en/content/articlehtml/2013/tb/c3tb20180e%20https://pubs.rsc.org/en/content/articlelanding/2013/tb/c3tb20180e

49. Negishi Y, Omata D, Iijima H, Hamano N, Endo-Takahashi Y, Nomizu M en Aramaki Y. Preparation and characterization of laminin-derived peptide AG73-coated liposomes as a selective gene delivery tool. Biological and Pharmaceutical Bulletin 2010; 33:1766–9. DOI: 10.1248/bpb.33.1766

50. Shaik F, Balderstone Michaela J, Arokiasamy S en Whiteford JR. Roles of Syndecan-4 in cardiac injury and repair. International Journal of Biochemistry and Cell Biology 2022; 146:106196. DOI: 10.1016/j.biocel.2022.106196. Available from: https://doi.org/10.1016/j.biocel.2022.106196

A Appendix

A.1 Experiment encapsulating C2C12

The mouse myoblast cell line C2C12 is encapsulated in the ALGAEMA hydrogel, since the C2C12 cells are commercially available at low cost, differentiate rapidly and behave consistently in cultures. This forms a model to study the effect of the RGD-peptides and dynamical properties of the hydrogel on myoblasts, the precursor cells of skeletal muscle cells.

The ALGAEMA and ALGAEMA-RGD prepared following Section 3.1 and 3.1.1 were used to prepare the conditions in Table 4. The ALGAEMA and ALGAEMA-RGD were functionalised with FGGC and CB[8] following Section 3.2.

Table 4: Different compositions of hydrogels using ALGAEMA and ALGAEMA-RGD for C2C12 encapsulation

Component	A	B	C	D	E
ALGAEMA	1	1	0	1	0
ALGAEMA-RGD	0	0	1	0	1
FGGC	0	1	1	1	1
CB[8]	0	0	0	1	1

C2C12 cells were kept frozen in liquid nitrogen and carried in ice when ready for use. After thawing in hot water (37 °C), the cells were added to 100 % FBS (Fetal Bovine Serum) and centrifuged (5 min at 1100 rounds per minute (rpm)). After the supernatant was removed and the pellet resuspended, the cells were added to a solution containing DMEM complete and FBS (1:10). The cells with the solution were put in a T25 culture flask and placed in the incubator (37 °)and left overnight to adhere and spread. The next day the cells were subcultured into a T75 and used when confluent.

After de DMEM was removed from the seeded C2C12 cells in the T75 culture flask, the C2C12 were washed with PBS. 2 mL Trypsin was added and set in the incubator for 3 minutes at 37 °C. The Trypsin action was stopped by adding 3 mL DMEM complete. The cells were resuspended and collected in a 15 mL tube before centrifuging for 5 min, 1100 (rpm). The supernatant was removed and the remained palet was resuspended in DMEM. The cells were counted using the EVE cell counter and a Trypan blue staining (NanoEntek, South Korea). In every hydrogel condition, 5 * 10^6 C2C12 cells were added and resuspended until the cells were homogeneously distributed in the hydrogel. 40 μL of the ALGAEMA-cell solution was transferred to a 5 mm diameter Ecoflex mould and UV-crosslinked for 1 minute and 30 seconds. After cross-linking the hydrogels were transferred to a 96-well plate and filled with 200 μL DMEM complete. A positive control with vitronectin was added to three wells as well. Every 48 hours the hydrogels were transferred to a new well, to get rid of the cells that leaked out of the hydrogel. 200 μL of DMEM was added again.

A.2 Experiment encapsulating hiPSC-CMs

The hiPSC-CMs are encapsulated in the ALGAEMA hydrogel to study 3D encapsulation possibilities with the presence of the synthetic laminin-α1 chain peptide AG73 (sequence FGGRKRLQVQLSIRT (residues 2719-2731, MW: 1757,05)) functionalised with Phe-GLy-GLy amino acids. AG73 is derived from the globular domain α1-LG4 and is known as a ligand to bind with Syndecan-1,4 [49] present in the cardiomyocytes [50].

The phenyl group of the Phe residue is utilized for participation in the host-guest system with CB[8] and in combination with the presence of FGGC, four different situations can occur, shown in Figure 18.

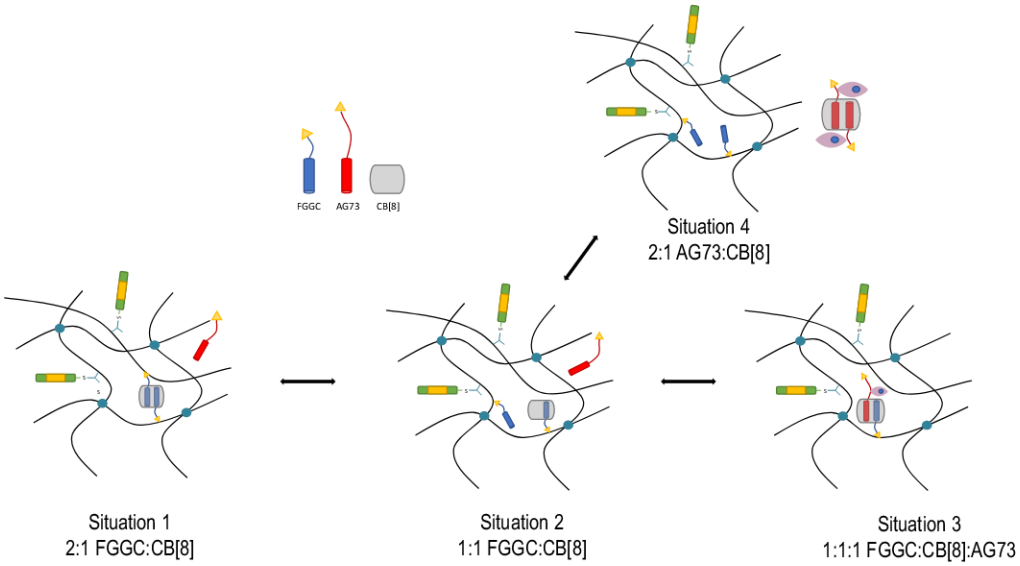

Figure 18: Possible situations that can occur after simultaneously adding two different peptides to the CB[8] cavity. The FGGC can bind to the alginate backbone and the AG73 contains a cell-binding sequence.

The ALGAEMA and ALGAEMA-RGD are prepared following Section 3.1 and 3.1.1 respectively. The formation of the hydrogel differs from Section 3.2 by dissolving 1mM of AG73 to 2mM of FGGC before dissolving 1mM CB[8] in the solution. The hydrogel precursor solutions were prepared following the conditions in Table 5. Each hydrogel contains 40 μL of 2% (w/v) ALGAEMA(-RGD) solution and every condition is executed in triplets. Before inserting the cells inside the hydrogel precursor, the hiPSC-CMs were prepared following Section 3.4.1

Table 5: Different conditions of hydrogels using ALGAEMA and ALGAEMA-RGD for hiPSC-CM encapsulation.

Component	A	B	C	D	E	F
ALGAEMA	1	0	0	0	1	0
ALGAEMA-RGD	0	1	1	1	0	1
FGGC	0	0	1	1	1	1
CB[8]	0	0	0	1	1	1

10μL of CM-DMEM containing a cell density of 2 * 10^5 cells/hydrogel was added to the hydrogel precursors and resuspended until the cells were homogeneously distributed in the hydrogel. 40 μL of the ALGAEMA-cell solution was transferred to a 5 mm diameter Ecoflex mould and UV-crosslinked for 1 minute and 30 seconds. After cross-linking the hydrogels were transferred to a 96-well plate and filled with 200 μL DMEM complete. Every 48 hours the hydrogels were transferred to a new well, to get rid of the cells that leaked out of the hydrogel. 200 μL of DMEM was added again.

A.3 Extended results of the stress relaxation measurement on the ALGAEMA FGGC hydrogel.

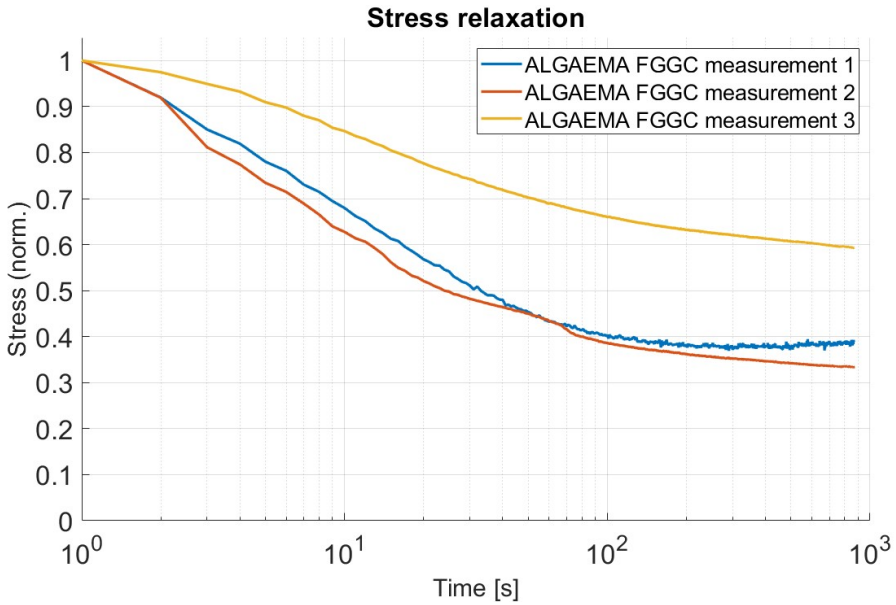

Figure 19: The results of the stress relaxation tests using rheology of every single ALGAEMA FGGC hydrogel. The $\tau = 1/2$ for measurement 1 is 33s, for measurement 2 is 24s and for measurement 3 is 861s.

A.4 Results positive control with fibrin

As a control for the quality of the hiPSC-CMs and a revision of the protocol, an experiment with a fibrin hydrogel was conducted. This hydrogel is a mixture of Matrigel and fibrin and is prepared according to the methods of the AST group of the University of Twente (Enschede, The Netherlands).

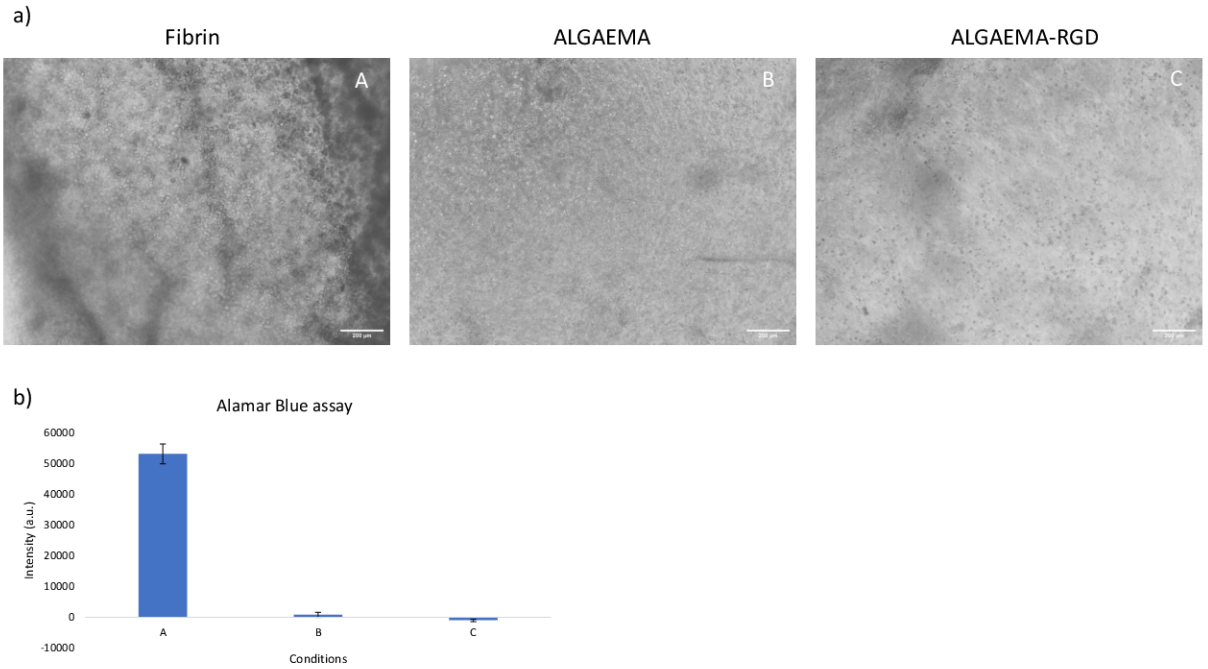

Figure 20: Results of encapsulated hiPSC-CMs in the fibrin hydrogel and the ALGAEMA-(RGD) hydrogel at day 1. a) The brightfield images of the hydrogels the day after encapsulation. b) The results of the Alamar Blue assay.

As shown in Figure 20b) the cell viability results of the encapsulated hiPSC-CMs indicate live cells after day 1 and non-living cells in the ALGAEMA and ALGAEMA-RGD hydrogels. After 6 days, the encapsulated cells showed observable beating, which could be observed by the brightfield microscope.

A.5 Additional results of surface seeding the hiPSC-CMs on the hydrogel with and without a pattern at day 3 and day 5 and the positive control.

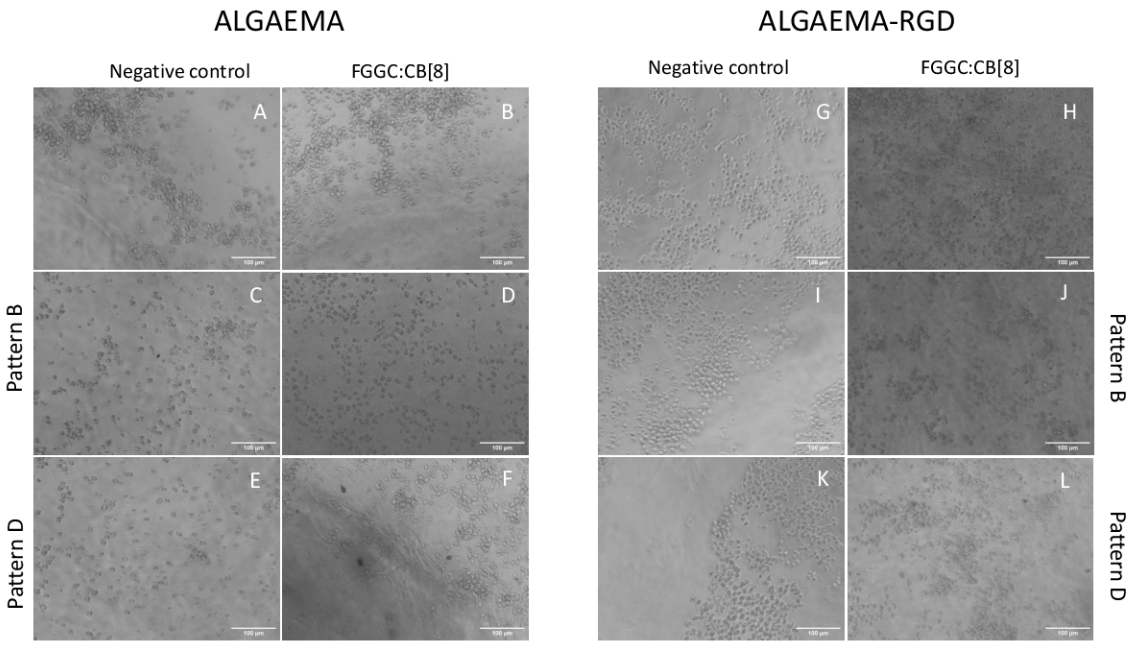

Figure 21: Brightfield images of the hiPSC-CMs seeded on the surface of the hydrogel at day 3. The images differ in terms of the composites of the hydrogel and the presence of a pattern on the surface. Pattern B contains grooves of 0,40 mm with a space of 0,20 mm between and pattern D contains 0,50 mm grooves with a space of 0,10 mm between (Figure 8).

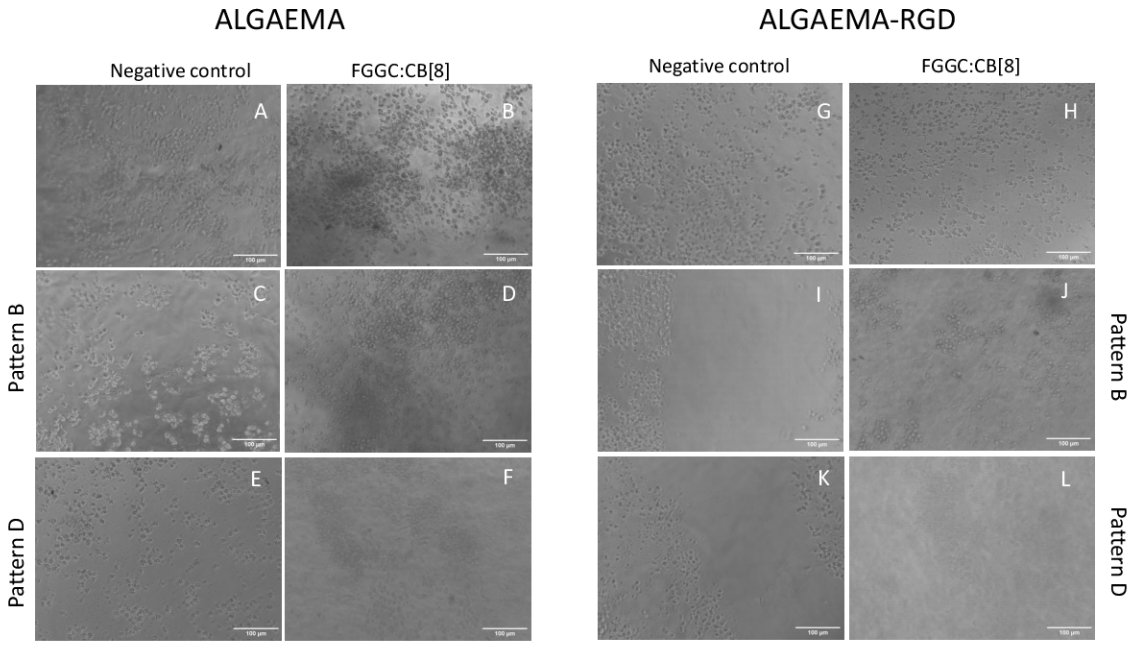

Figure 22: Brightfield images of the hiPSC-CMs seeded on the surface of the hydrogel at day 5. The images differ in terms of the composites of the hydrogel and the presence of a pattern on the surface. Pattern B contains grooves of 0,40 mm with a space of 0,20 mm between and pattern D contains 0,50 mm grooves with a space of 0,10 mm between (Figure 8).

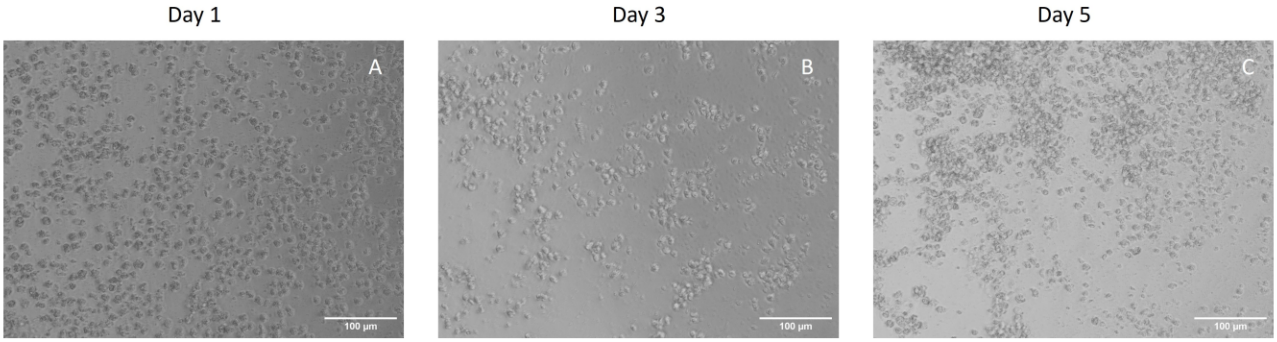

Figure 23: Brightfield images of the hiPSC-CMs seeded on a Matrigel-coated well plate at day 1, day 3 and day 5.

A.6 Matlab script for processing time sweep data obtained with rheology.

```
    clear all
close all
clc
%% Conditie A
pname = 'Z:\Matlab_script'; %file location, you can use same ...
   pname for all files (if in same location)
fname_A1 = ...
   '17102023_2%ALGAEMA0,1%LAP_timesweep_1_4723.xls';%file name
fullpath_A1 = fullfile(pname,fname_A1); %niet aanpassen
A1=readtable(fullpath_A1,'sheet', 'Time sweep - 1', ...
   'VariableNamingRule', 'preserve' );%change name sheet if ...
   required
A1_s = A1{:,["Storage modulus"]};
A1_s = A1_s(2:16,:); %36 handmatig aanpassen
A1_sm = mean(A1_s);
A1_ss = std(A1_s);
A1_l = A1{:,["Loss modulus"]};
A1_l = A1_l(2:16,:); %36 handmatig aanpassen
A1_lm = mean(A1_l);
A1_ls = std(A1_l);
fname_A2 = ...
   '17102023_2%ALGAEMA0,1%LAP_timesweep_2aaa_4738.xls';%file name
fullpath_A2 = fullfile(pname,fname_A2); %niet aanpassen
A2=readtable(fullpath_A2,'sheet', 'Time sweep - 1', ...
   'VariableNamingRule', 'preserve' );%change name sheet if ...
   required
A2_s = A2{:,["Storage modulus"]};
A2_s = A2_s(2:15,:); %36 handmatig aanpassen
A2_sm = mean(A2_s);
A2_ss = std(A2_s);
A2_l = A2{:,["Loss modulus"]};
A2_l = A2_l(2:15,:); %36 handmatig aanpassen
A2_lm = mean(A2_l);
A2_ls = std(A2_l);
fname_A3 = ...
   '17102023_2%ALGAEMA0,1%LAP_timesweep_3_4740.xls';%file name
fullpath_A3 = fullfile(pname,fname_A3); %niet aanpassen
A3=readtable(fullpath_A3,'sheet', 'Time sweep - 1', ...
   'VariableNamingRule', 'preserve' );%change name sheet if ...
   required
A3_s = A3{:,["Storage modulus"]};
A3_s = A3_s(2:15,:); %36 handmatig aanpassen
A3_sm = mean(A3_s);
A3_ss = std(A3_s);
A3_l = A3{:,["Loss modulus"]};
A3_l = A3_l(2:15,:); %36 handmatig aanpassen
A3_lm = mean(A3_l);
A3_ls = std(A3_l);
Asm = mean([A1_sm A2_sm A3_sm]);
Ass = sqrt([A1_ss^2 + A2_ss^2 + A3_ss^2]);
```

```
Alm = mean([A1_lm A2_lm A3_lm]);
Als = sqrt([A1_ls^2 + A2_ls^2 + A3_ls^2]);
%% conditie B
fname_B1 = ...
    '17102023_2%ALGAEMA0,1%LAP_RGD_FGGC_timesweep_1_4725';%file ...
    name
fullpath_B1 = fullfile(pname,fname_B1); %niet aanpassen
B1=readtable(fullpath_B1,'sheet', 'Time sweep - 1', ...
    'VariableNamingRule', 'preserve' );%change name sheet if ...
    required
B1_s = B1{:,["Storage modulus"]};
B1_s = B1_s(2:15,:); %36 handmatig aanpassen
B1_sm = mean(B1_s);
B1_ss = std(B1_s);
B1_l = B1{:,["Loss modulus"]};
B1_l = B1_l(2:15,:); %36 handmatig aanpassen
B1_lm = mean(B1_l);
B1_ls = std(B1_l);
fname_B2 = ...
    '17102023_2%ALGAEMA0,1%LAP_RGD_FGGC_timesweep_2_4742';%file ...
    name
fullpath_B2 = fullfile(pname,fname_B2); %niet aanpassen
B2=readtable(fullpath_B2,'sheet', 'Time sweep - 1', ...
    'VariableNamingRule', 'preserve' );%change name sheet if ...
    required
B2_s = B2{:,["Storage modulus"]};
B2_s = B2_s(2:15,:); %36 handmatig aanpassen
B2_sm = mean(B2_s);
B2_ss = std(B2_s);
B2_l = B2{:,["Loss modulus"]};
B2_l = B2_l(2:15,:); %36 handmatig aanpassen
B2_lm = mean(B2_l);
B2_ls = std(B2_l);
pname = 'Z:\Matlab_script'; %file location, you can use same ...
    pname for all files (if in same location)
fname_B3 = ...
    '17102023_2%ALGAEMA0,1%LAP_RGD_FGGC_timesweep_3_4744';%file ...
    name
fullpath_B3 = fullfile(pname,fname_B3); %niet aanpassen
B3=readtable(fullpath_B3,'sheet', 'Time sweep - 1', ...
    'VariableNamingRule', 'preserve' );%change name sheet if ...
    required
B3_s = B3{:,["Storage modulus"]};
B3_s = B3_s(2:15,:); %36 handmatig aanpassen
B3_sm = mean(B3_s);
B3_ss = std(B3_s);
B3_l = B3{:,["Loss modulus"]};
B3_l = B3_l(2:15,:); %36 handmatig aanpassen
B3_lm = mean(B3_l);
B3_ls = std(B3_l);
Bsm = mean([B1_sm B2_sm B3_sm]);
Bss = sqrt([B1_ss^2 + B2_ss^2 + B3_ss^2]);
```

```
80 Blm = mean([B1_lm B2_lm B3_lm]);
81 Bls = sqrt([B1_ls^2 + B2_ls^2 + B3_ls^2]);
82
83 %% Conditie C
84 fname_C1 = ...
      '17102023_2%ALGAEMA0,1%LAP_FGGC_timesweep_1_4727';%file name
85 fullpath_C1 = fullfile(pname,fname_C1); %niet aanpassen
86 C1=readtable(fullpath_C1,'sheet', 'Time sweep - 1', ...
      'VariableNamingRule', 'preserve' );%change name sheet if ...
      required
87 C1_s = C1{:,["Storage modulus"]};
88 C1_s = C1_s(2:15,:); %36 handmatig aanpassen
89 C1_sm = mean(C1_s);
90 C1_ss = std(C1_s);
91 C1_l = C1{:,["Loss modulus"]};
92 C1_l = C1_l(2:15,:); %36 handmatig aanpassen
93 C1_lm = mean(C1_l);
94 C1_ls = std(C1_l);
95 fname_C2 = ...
      '17102023_2%ALGAEMA0,1%LAP_FGGC_timeseep_2_4746';%file name
96 fullpath_C2 = fullfile(pname,fname_C2); %niet aanpassen
97 C2=readtable(fullpath_C2,'sheet', 'Time sweep - 1', ...
      'VariableNamingRule', 'preserve' );%change name sheet if ...
      required
98 C2_s = C2{:,["Storage modulus"]};
99 C2_s = C2_s(2:15,:); %36 handmatig aanpassen
100 C2_sm = mean(C2_s);
101 C2_ss = std(C2_s);
102 C2_l = C2{:,["Loss modulus"]};
103 C2_l = C2_l(2:15,:); %36 handmatig aanpassen
104 C2_lm = mean(C2_l);
105 C2_ls = std(C2_l);
106 fname_C3 = ...
      '17102023_2%ALGAEMA0,1%LAP_FGGC_timesweep_3_4748';%file name
107 fullpath_C3 = fullfile(pname,fname_C3); %niet aanpassen
108 C3=readtable(fullpath_C3,'sheet', 'Time sweep - 1', ...
      'VariableNamingRule', 'preserve' );%change name sheet if ...
      required
109 C3_s = C3{:,["Storage modulus"]};
110 C3_s = C3_s(2:15,:); %36 handmatig aanpassen
111 C3_sm = mean(C3_s);
112 C3_ss = std(C3_s);
113 C3_l = C3{:,["Loss modulus"]};
114 C3_l = C3_l(2:15,:); %36 handmatig aanpassen
115 C3_lm = mean(C3_l);
116 C3_ls = std(C3_l);
117 Csm = mean([C1_sm C2_sm C3_sm]);
118 Css = sqrt([C1_ss^2 + C2_ss^2 + C3_ss^2]);
119 Clm = mean([C1_lm C2_lm C3_lm]);
120 Cls = sqrt([C1_ls^2 + C2_ls^2 + C3_ls^2]);
121
122
```

```
%% Condition D
pname = 'Z:\Matlab_script'; %file location, you can use same ...
    pname for all files (if in same location)
fname_D1 = ...
    '17102023_2%ALGAEMA0,1%LAP_FGGC_CB8_timesweep_1a_4730';%file ...
    name
fullpath_D1 = fullfile(pname,fname_D1); %niet aanpassen
D1=readtable(fullpath_D1,'sheet', 'Time sweep - 1', ...
    'VariableNamingRule', 'preserve' );%change name sheet if ...
    required
D1_s = D1{:,["Storage modulus"]};
D1_s = D1_s(2:15,:); %36 handmatig aanpassen
D1_sm = mean(D1_s);
D1_ss = std(D1_s);
D1_l = D1{:,["Loss modulus"]};
D1_l = D1_l(2:15,:); %36 handmatig aanpassen
D1_lm = mean(D1_l);
D1_ls = std(D1_l);
fname_D2 = ...
    '17102023_2%ALGAEMA0,1%LAP_FGGC_CB8_timesweep_2a_4751';%file ...
    name
fullpath_D2 = fullfile(pname,fname_D2); %niet aanpassen
D2=readtable(fullpath_D2,'sheet', 'Time sweep - 1', ...
    'VariableNamingRule', 'preserve' );%change name sheet if ...
    required
D2_s = D2{:,["Storage modulus"]};
D2_s = D2_s(2:15,:); %36 handmatig aanpassen
D2_sm = mean(D2_s);
D2_ss = std(D2_s);
D2_l = D2{:,["Loss modulus"]};
D2_l = D2_l(2:15,:); %36 handmatig aanpassen
D2_lm = mean(D2_l);
D2_ls = std(D2_l);

Dsm = mean([D1_sm D2_sm ]);
Dss = sqrt([D1_ss^2 + D2_ss^2 ]);
Dlm = mean([D1_lm D2_lm ]);
Dls = sqrt([D1_ls^2 + D2_ls^2 ]);

%% Condition E
pname = 'Z:\Matlab_script'; %file location, you can use same ...
    pname for all files (if in same location)
fname_E1 = ...
    '17102023_2%ALGAEMA0,1%LAP_RGD_FGGC_CB8_timesweep_1a_4733';%file ...
    name
fullpath_E1 = fullfile(pname,fname_E1); %niet aanpassen
E1=readtable(fullpath_E1,'sheet', 'Time sweep - 1', ...
    'VariableNamingRule', 'preserve' );%change name sheet if ...
    required
E1_s = E1{:,["Storage modulus"]};
E1_s = E1_s(2:15,:); %36 handmatig aanpassen
E1_sm = mean(E1_s);
```

```
E1_ss = std(E1_s);
E1_l = E1{:,["Loss modulus"]};
E1_l = E1_l(2:15,:); %36 handmatig aanpassen
E1_lm = mean(E1_l);
E1_ls = std(E1_l);
fname_E2 = ...
    '17102023_2%ALGAEMA0,1%LAP_RGD_FGGC_CB8_timesweep_2_4756';%file ...
    name
fullpath_E2 = fullfile(pname,fname_E2); %niet aanpassen
E2=readtable(fullpath_E2,'sheet', 'Time sweep - 1', ...
    'VariableNamingRule', 'preserve' );%change name sheet if ...
    required
E2_s = E2{:,["Storage modulus"]};
E2_s = E2_s(2:15,:); %36 handmatig aanpassen
E2_sm = mean(E2_s);
E2_ss = std(E2_s);
E2_l = E2{:,["Loss modulus"]};
E2_l = E2_l(2:15,:); %36 handmatig aanpassen
E2_lm = mean(E2_l);
E2_ls = std(E2_l);
fname_E3 = ...
    '17102023_2%ALGAEMA0,1%LAP_RGD_FGGC_CB8_timesweep_3_4758';%file ...
    name
fullpath_E3 = fullfile(pname,fname_E3); %niet aanpassen
E3=readtable(fullpath_E3,'sheet', 'Time sweep - 1', ...
    'VariableNamingRule', 'preserve' );%change name sheet if ...
    required
E3_s = E3{:,["Storage modulus"]};
E3_s = E3_s(2:15,:); %36 handmatig aanpassen
E3_sm = mean(E3_s);
E3_ss = std(E3_s);
E3_l = E3{:,["Loss modulus"]};
E3_l = E3_l(2:15,:); %36 handmatig aanpassen
E3_lm = mean(E3_l);
E3_ls = std(E3_l);
Esm = mean([E1_sm E2_sm E3_sm]);
Ess = sqrt([E1_ss^2 + E2_ss^2 + E3_ss^2]);
Elm = mean([E1_lm E2_lm E3_lm]);
Els = sqrt([E1_ls^2 + E2_ls^2 + E3_ls^2]);

%%
y = [Asm Alm Bsm Blm Csm Clm Dsm Dlm Esm Elm];
ys = [Ass Als Bss Bls Css Cls Dss Dls Ess Els];
%%
f= figure(1)
clf(1), hold on
hBar = bar(diag(y,0),'stacked');
oddColor = [0.3010 0.7450 0.9330];
evenColor = [0.9290 0.6940 0.1250];
for i = 1:length(y)
    if mod(i, 2) ~= 0
        hBar(i).FaceColor = oddColor;
```

```
    else
        hBar(i).FaceColor = evenColor;
    end
end
errorbar(y,ys, '.k')
hold off
PPx=categorical({'ALGAEMA','ALGAEMA-RGD FGGC', 'ALGAEMA FGGC', ...
   'ALGAEMA FGGC:CB[8]','ALGAEMA-RGD FGGC:CB[8]'}); %for names ...
   under x-axis
XTick=1.5:2:9.5;
set(gca, 'XTick',XTick);
set(gca, 'XTickLabel', PPx) %can be used if you want text
%instead of numbers at x-axis
legend('G''','G"','Location','northeast') %legend has to be ...
   outside of graph
title('Time sweep')
ylabel('Modulus (Pa)')
saveas(figure(1),[pwd,'Irradiation and time sweep ...
   20231013.jpeg']) %can specify where to save figure
```

A.7 Matlab script for processing stress relaxation data obtained with rheology.

```
    clear, clc
pname = 'Z:\Matlab_script\stress_relaxation'; %file location, ...
   you can use same pname for all files (if in same location)
% A1, A2, A3, B1, B2, ....
fname = {'17102023_2%ALGAEMA0,1%LAP_stressrelaxation_1_4724.xls';
    '17102023_2%ALGAEMA0,1%LAP_stressrelaxation_2aaa_4739.xls';
    '17102023_2%ALGAEMA0,1%LAP_stressrelaxation_3_4741.xls';
    '17102023_2%ALGAEMA0,1%LAP_RGD_FGGC_stressrelaxation_1_4726';
    '17102023_2%ALGAEMA0,1%LAP_RGD_FGGC_stressrelaxation_2_4743';
    '17102023_2%ALGAEMA0,1%LAP_RGD_FGGC_stressrelaxation_3_4745';
    '17102023_2%ALGAEMA0,1%LAP_FGGC_stressrelaxation_1_4728';
    '17102023_2%ALGAEMA0,1%LAP_FGGC_stressrelaxation_2_4747' ;
    '17102023_2%ALGAEMA0,1%LAP_FGGC_stressrelaxation_3_4749';
    '17102023_2%ALGAEMA0,1%LAP_FGGC_CB8_stressrelaxation_1_4731';
    '17102023_2%ALGAEMA0,1%LAP_FGGC_CB8_stressrelaxation_2a_4752';
    '17102023_2%ALGAEMA0,1%LAP_FGGC_CB8_stressrelaxation_3a_4755';
    '17102023_2%ALGAEMA0,1%LAP_RGD_FGGC_CB8_stressrelaxation_1_4734';
    '17102023_2%ALGAEMA0,1%LAP_RGD_FGGC_CB8_stressrelaxation_2_4757';
    '17102023_2%ALGAEMA0,1%LAP_RGD_FGGC_CB8_stressrelaxation_3_4759'};%file
       name
for i = 1:size(fname,1)
    fullpath = fullfile(pname,fname(i)); %niet aanpassen
    max_size(:,i) = size(readtable(char(fullpath),'sheet', ...
       'Stress relaxation - 1', 'VariableNamingRule', ...
       'preserve' ).Stressnormalized,1);%change name sheet if ...
       required
end
Stressnormalized_val = zeros(max(max_size),size(fname,1));
for i = 1:size(fname,1)
```

```
25      fullpath = fullfile(pname,fname(i)); %niet aanpassen
26      Stressnormalized = readtable(char(fullpath),'sheet', ...
            'Stress relaxation - 1', 'VariableNamingRule', ...
            'preserve' ).Stressnormalized;%change name sheet if ...
            required
27      Stressnormalized_val(1:length(Stressnormalized),i) = ...
            Stressnormalized;
28  end
29  Stressnormalized_val_resize = Stressnormalized_val(1:867,:);
30  time_vec = 1:867;
31  A_mean = mean(Stressnormalized_val_resize(:,1:3),2);
32  [¬,idx]=min(abs(A_mean-A_mean(1)/2));
33  A_half = time_vec(idx);
34
35  B_mean = mean(Stressnormalized_val_resize(:,4:6),2);
36  [¬,idx]=min(abs(B_mean-B_mean(1)/2));
37  B_half = time_vec(idx);
38
39  C_mean = mean(Stressnormalized_val_resize(:,7:9),2);
40  [¬,idx]=min(abs(C_mean-C_mean(1)/2));
41  C_half = time_vec(idx);
42
43  D_mean = mean(Stressnormalized_val_resize(:,10:12),2);
44  [¬,idx]=min(abs(D_mean-D_mean(1)/2));
45  D_half = time_vec(idx);
46
47  E_mean = mean(Stressnormalized_val_resize(:,13:15),2);
48  [¬,idx]=min(abs(E_mean-E_mean(1)/2));
49  E_half = time_vec(idx);
50
51  time_line = [A_half,B_half,C_half,D_half,E_half];
52
53  plotID = 1;
54  f = figure(plotID);
55  LineWidth = 2
56  clf(plotID);
57  set(plotID, 'Position', [0 20 1000 600], 'defaultaxesfontsize', ...
        18, 'defaulttextfontsize', 18, 'PaperPositionMode', 'auto');
58  hold on;
59  grid on;
60  title("Stress relaxation",'FontSize',22);
61  plot(time_vec,A_mean,time_vec,B_mean,time_vec,C_mean,time_vec,D_mean,time_ve
        'LineWidth',LineWidth)
62
63
64  set(findall(gcf,'-property','FontSize'),'FontSize',20)
65  legend({'ALGAEMA','ALGAEMA-RGD FGGC','ALGAEMA FGGC','ALGAEMA ...
        FGGC:CB[8]','ALGAEMA-RGD FGGC:CB[8]'}, 'Location', ...
        'northeast','FontSize',16);
66  xlabel('Time [s]','FontSize',18);
67  xscale("log")
68  ylabel('Stress (norm.)','FontSize',18);
```

```
69 yticks(0:0.1:1)
70 ylim([0,1.05])
71 hold off
```

A.8 Matlab script for visualizing the Youngs modulus.

```
    clear all
close all
clc
%% Conditie A
pname = 'Z:\Matlab_script'; %file location, you can use same ...
   pname for all files (if in same location)
fname_A1 = ...
   '17102023_2%ALGAEMA0,1%LAP_timesweep_1_4723.xls';%file name
fullpath_A1 = fullfile(pname,fname_A1); %niet aanpassen
A1=readtable(fullpath_A1,'sheet', 'Time sweep - 1', ...
   'VariableNamingRule', 'preserve' );%change name sheet if ...
   required
A1_c = A1{:,["Youngs modulus"]};
A1_c = A1_c(2:16,:); %36 handmatig aanpassen
A1_cm = mean(A1_c);
A1_cs = std(A1_c);
fname_A2 = ...
   '17102023_2%ALGAEMA0,1%LAP_timesweep_2aaa_4738.xls';%file name
fullpath_A2 = fullfile(pname,fname_A2); %niet aanpassen
A2=readtable(fullpath_A2,'sheet', 'Time sweep - 1', ...
   'VariableNamingRule', 'preserve' );%change name sheet if ...
   required
A2_c = A2{:,["Youngs modulus"]};
A2_c = A2_c(2:15,:); %36 handmatig aanpassen
A2_cm = mean(A2_c);
A2_cs = std(A2_c);
fname_A3 = ...
   '17102023_2%ALGAEMA0,1%LAP_timesweep_3_4740.xls';%file name
fullpath_A3 = fullfile(pname,fname_A3); %niet aanpassen
A3=readtable(fullpath_A3,'sheet', 'Time sweep - 1', ...
   'VariableNamingRule', 'preserve' );%change name sheet if ...
   required
A3_c = A3{:,["Youngs modulus"]};
A3_c = A3_c(2:15,:); %36 handmatig aanpassen
A3_cm = mean(A3_c);
A3_cs = std(A3_c);
Acm = mean([A1_cm A2_cm A3_cm]);
Acs = sqrt([A1_cs^2 + A2_cs^2 + A3_cs^2]);
%% conditie B
fname_B1 = ...
   '17102023_2%ALGAEMA0,1%LAP_RGD_FGGC_timesweep_1_4725';%file ...
   name
fullpath_B1 = fullfile(pname,fname_B1); %niet aanpassen
B1=readtable(fullpath_B1,'sheet', 'Time sweep - 1', ...
   'VariableNamingRule', 'preserve' );%change name sheet if ...
   required
B1_c = B1{:,["Youngs modulus"]};
B1_c = B1_c(2:15,:); %36 handmatig aanpassen
B1_cm = mean(B1_c);
B1_cs = std(B1_c);
```

```
fname_B2 = ...
    '17102023_2%ALGAEMA0,1%LAP_RGD_FGGC_timesweep_2_4742';%file ...
    name
fullpath_B2 = fullfile(pname,fname_B2); %niet aanpassen
B2=readtable(fullpath_B2,'sheet', 'Time sweep - 1', ...
    'VariableNamingRule', 'preserve' );%change name sheet if ...
    required
B2_c = B2{:,["Youngs modulus"]};
B2_c = B2_c(2:15,:); %36 handmatig aanpassen
B2_cm = mean(B2_c);
B2_cs = std(B2_c);
pname = 'Z:\Matlab_script'; %file location, you can use same ...
    pname for all files (if in same location)
fname_B3 = ...
    '17102023_2%ALGAEMA0,1%LAP_RGD_FGGC_timesweep_3_4744';%file ...
    name
fullpath_B3 = fullfile(pname,fname_B3); %niet aanpassen
B3=readtable(fullpath_B3,'sheet', 'Time sweep - 1', ...
    'VariableNamingRule', 'preserve' );%change name sheet if ...
    required
B3_c = B3{:,["Youngs modulus"]};
B3_c = B3_c(2:15,:); %36 handmatig aanpassen
B3_cm = mean(B3_c);
B3_cs = std(B3_c);
Bcm = mean([B1_cm B2_cm B3_cm]);
Bcs = sqrt([B1_cs^2 + B2_cs^2 + B3_cs^2])
%% Conditie C
fname_C1 = ...
    '17102023_2%ALGAEMA0,1%LAP_FGGC_timesweep_1_4727';%file name
fullpath_C1 = fullfile(pname,fname_C1); %niet aanpassen
C1=readtable(fullpath_C1,'sheet', 'Time sweep - 1', ...
    'VariableNamingRule', 'preserve' );%change name sheet if ...
    required
C1_c = C1{:,["Youngs modulus"]};
C1_c = C1_c(2:15,:); %36 handmatig aanpassen
C1_cm = mean(C1_c);
C1_cs = std(C1_c);
fname_C2 = ...
    '17102023_2%ALGAEMA0,1%LAP_FGGC_timeseep_2_4746';%file name
fullpath_C2 = fullfile(pname,fname_C2); %niet aanpassen
C2=readtable(fullpath_C2,'sheet', 'Time sweep - 1', ...
    'VariableNamingRule', 'preserve' );%change name sheet if ...
    required
C2_c = C2{:,["Youngs modulus"]};
C2_c = C2_c(2:15,:); %36 handmatig aanpassen
C2_cm = mean(C2_c);
C2_cs = std(C2_c);
fname_C3 = ...
    '17102023_2%ALGAEMA0,1%LAP_FGGC_timesweep_3_4748';%file name
fullpath_C3 = fullfile(pname,fname_C3); %niet aanpassen
```

```
71 C3=readtable(fullpath_C3,'sheet', 'Time sweep - 1', ...
      'VariableNamingRule', 'preserve' );%change name sheet if ...
      required
72 C3_c = C3{:,["Youngs modulus"]};
73 C3_c = C3_c(2:15,:); %36 handmatig aanpassen
74 C3_cm = mean(C3_c);
75 C3_cs = std(C3_c);
76 Ccm = mean([C1_cm C2_cm C3_cm]);
77 Ccs = sqrt([C1_cs^2 + C2_cs^2 + C3_cs^2]);
78 %% Condition D
79 pname = 'Z:\Matlab_script'; %file location, you can use same ...
      pname for all files (if in same location)
80 fname_D1 = ...
      '17102023_2%ALGAEMA0,1%LAP_FGGC_CB8_timesweep_1a_4730';%file ...
      name
81 fullpath_D1 = fullfile(pname,fname_D1); %niet aanpassen
82 D1=readtable(fullpath_D1,'sheet', 'Time sweep - 1', ...
      'VariableNamingRule', 'preserve' );%change name sheet if ...
      required
83 D1_c = D1{:,["Youngs modulus"]};
84 D1_c = D1_c(2:15,:); %36 handmatig aanpassen
85 D1_cm = mean(D1_c);
86 D1_cs = std(D1_c);
87 fname_D2 = ...
      '17102023_2%ALGAEMA0,1%LAP_FGGC_CB8_timesweep_2a_4751';%file ...
      name
88 fullpath_D2 = fullfile(pname,fname_D2); %niet aanpassen
89 D2=readtable(fullpath_D2,'sheet', 'Time sweep - 1', ...
      'VariableNamingRule', 'preserve' );%change name sheet if ...
      required
90 D2_c = D2{:,["Youngs modulus"]};
91 D2_c = D2_c(2:15,:); %36 handmatig aanpassen
92 D2_cm = mean(D2_c);
93 D2_cs = std(D2_c);
94 Dcm = mean([D1_cm D2_cm ]);
95 Dcs = sqrt([D1_cs^2 + D2_cs^2 ]);
96 %% Condition E
97 pname = 'Z:\Matlab_script'; %file location, you can use same ...
      pname for all files (if in same location)
98 fname_E1 = ...
      '17102023_2%ALGAEMA0,1%LAP_RGD_FGGC_CB8_timesweep_1a_4733';%file ...
      name
99 fullpath_E1 = fullfile(pname,fname_E1); %niet aanpassen
100 E1=readtable(fullpath_E1,'sheet', 'Time sweep - 1', ...
      'VariableNamingRule', 'preserve' );%change name sheet if ...
      required
101 E1_c = E1{:,["Youngs modulus"]};
102 E1_c = E1_c(2:15,:); %36 handmatig aanpassen
103 E1_cm = mean(E1_c);
104 E1_cs = std(E1_c);
```

```
fname_E2 = ...
    '17102023_2%ALGAEMA0,1%LAP_RGD_FGGC_CB8_timesweep_2_4756';%file ...
    name
fullpath_E2 = fullfile(pname,fname_E2); %niet aanpassen
E2=readtable(fullpath_E2,'sheet', 'Time sweep - 1', ...
    'VariableNamingRule', 'preserve' );%change name sheet if ...
    required
E2_c = E2{:,["Youngs modulus"]};
E2_c = E2_c(2:15,:); %36 handmatig aanpassen
E2_cm = mean(E2_c);
E2_cs = std(E2_c);
fname_E3 = ...
    '17102023_2%ALGAEMA0,1%LAP_RGD_FGGC_CB8_timesweep_3_4758';%file ...
    name
fullpath_E3 = fullfile(pname,fname_E3); %niet aanpassen
E3=readtable(fullpath_E3,'sheet', 'Time sweep - 1', ...
    'VariableNamingRule', 'preserve' );%change name sheet if ...
    required
E3_c = E3{:,["Youngs modulus"]};
E3_c = E3_c(2:15,:); %36 handmatig aanpassen
E3_cm = mean(E3_c);
E3_cs = std(E3_c);
Ecm = mean([E1_cm E2_cm E3_cm]);
Ecs = sqrt([E1_cs^2 + E2_cs^2 + E3_cs^2]);
%%
y = [Acm Bcm Ccm Dcm Ecm];
ys = [Acs Bcs Ccs Dcs Ecs];
%%
f= figure(1)
clf(1), hold on
hBar = bar(diag(y,0),'stacked','FaceColor',[0.4660 0.6740 ...
    0.1880]);
errorbar(y,ys, '.k')
hold off
PPx=categorical({'ALGAEMA','ALGAEMA-RGD FGGC', 'ALGAEMA FGGC', ...
    'ALGAEMA FGGC:CB[8]','ALGAEMA-RGD FGGC:CB[8]'}); %for names ...
    under x-axis
XTick=1:1:5
set(gca, 'XTick',XTick);
set(gca, 'XTickLabel', PPx) %can be used if you want text
%instead of numbers at x-axis
title('Youngs modulus')
ylabel('Modulus (Pa)')
saveas(figure(1),[pwd,'Irradiation and time sweep ...
    20231013.jpeg']) %can specify where to save figure
```